Roles of Embryonic Hindgut Endoderm in Primordial Germ Cells Migration and Differentiation in Mice

（マウス始原生殖細胞の移動および分化における胚性内胚葉の役割について）

Kenshiro Hara

原　健士朗

Contents

1. General Introduction

In most animals, primordial germ cells (PGCs) arise very early in development at a site distinct from which gonads are ultimately formed. PGCs migrate through various tissues of the embryo toward genital ridges (GRs) during embryogenensis. Then, they form eggs and sperm in adult. They are the only cells in the body to undergo meiosis. Therefore, PGCs migration and differentiation are essential for gametogenesis and insure a series of life cycle of each species. In contrast, ectopic PGCs are also found mainly due to the failure of PGCs migration, and they potentially cause the malignant pediatric or adult tumors. Therefore, elucidation of the mechanisms of mammalian PGCs migration and differentiation is a quite important subject for developmental biology.

In mammalian model, mouse, PGCs arise around gastrulation between 6.25 and 7 days post coitum (dpc) from a pluripotent population of cells in the proximal epiblast (McLaren and Lawson, 2005; Ohinata *et al*., 2005). The germ cell lineage is discriminated from somatic cell lineage during development, and repression of the somatic cell fate is therefore a key event during the germ cell specification. The specification is initiated by signals provided by the extraembryonic ectoderm, and the visceral endoderm that surrounds the epiblast cells and instructs a small population of epiblast cells to become PGCs (Lawson *et al.,* 1999; Ying *et al.,* 2000). Blimp1 is a key transcriptional regulator that is partly responsible for repressing the somatic program in PGCs (Ohinata *et al.,* 2005). In *Blimp1*-expressing cells, pluripotency-associated genes such as *Nanog* (Yamaguchi *et al.,* 2005) and *Oct4*

(Schöler *et al.,* 1990), in addition to other unique genes in PGCs such as *PGC7* (*Stella, Dppa3*) (Saitou *et al.,* 2002; Sato *et al.,* 2002) and *Ifitm3* (*Fragilis, mil1*) (Saitou *et al.,* 2002; Tanaka and Matsui, 2002), are up-regulated. Specified PGCs migrate through the primitive streak into the region of the embryonic endoderm that forms the hindgut (7.5~8.5 dpc). Later in development between 8.5 and 9.5 dpc, the second phase of migration takes place in which PGCs migrate randomly within the hindgut epithelium (Anderson *et al.,* 2000). Finally, between 9.5 and 10.5 dpc, PGCs emerging from the hindgut are seen in the dorsal mesentery and migrate into two bilateral streams towards the GRs (Molyneaux *et al.,* 2001; 2003).

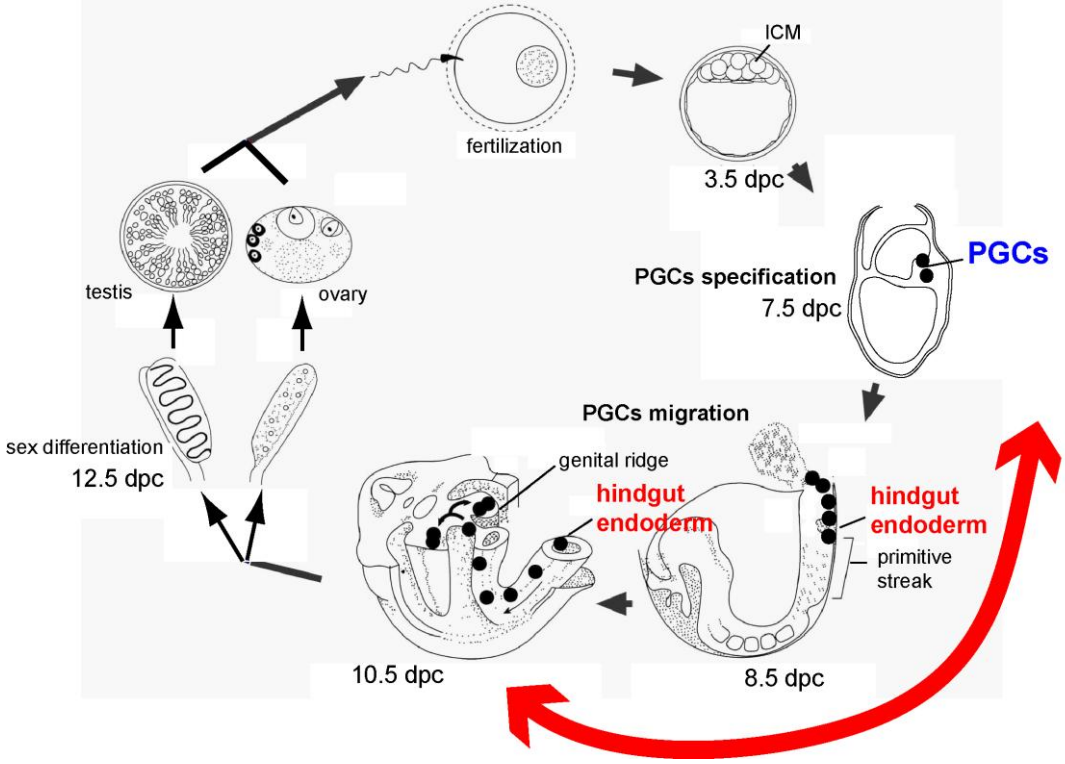

Figure 1-1. **PGCs migration within the embryonic hindgut endoderm in germ cell development in mouse embryogenesis.** Red double-headed arrow indicates the period of PGCs migration within the embryonic hindgut endoderm.

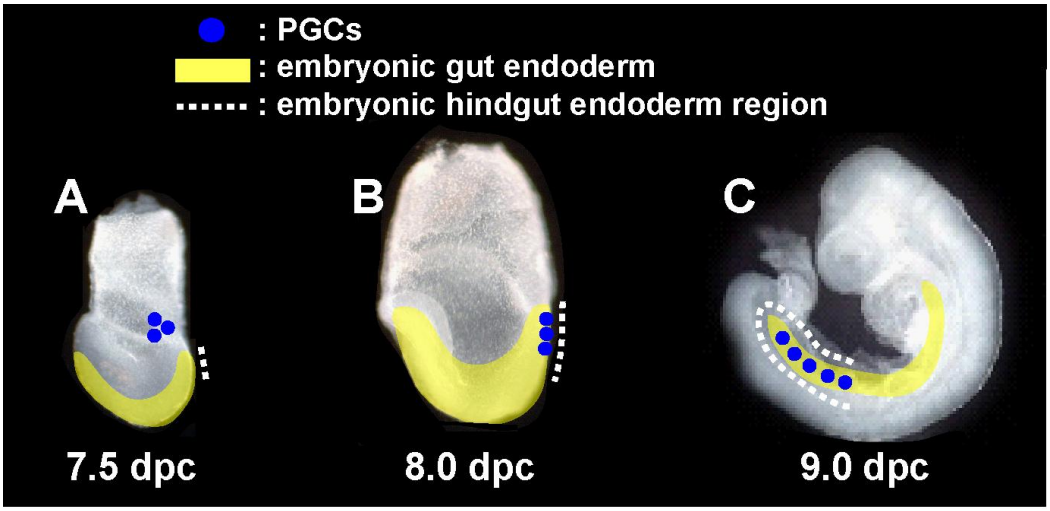

Figure 1-2. **PGCs and embryonic hindgut endoderm regionalization during dynamic morphogenesis in mouse.**

(A~C) Lateral views of mouse embryo at 7.5 (A), 8.0 (B), and 9.0 dpc (C). PGCs are formed at around 7.5 dpc in the extraembryonic base of allantois (A). At around 8.0 dpc, PGCs invade the embryonic hindgut endoderm layer that will form the hindgut tube (B). The bridled embryo undergo turning, and then hindgut tube is formed during 8.0 and 9.0 dpc (B, C). During these morphogenesis, PGCs localize within the embryonic hindgut endoderm tissue (B, C).

As described above, it requires two days out of the total three-day-migration period for PGCs to migrate through the embryonic hindgut endoderm toward GRs in mouse embryogenesis (Fig. 1-1 and Fig. 1-2). How and why do they migrate within the embryonic hindgut endoderm? In several vertebrates including zebrafish, medaka, chicken, and mouse, recent studies have shown that PGCs migration toward the

GRs depends on the activity of the chemokine receptor CXCR4, and its SDF-1 ligand (Doitsidou *et al.,* 2002; Ara *et al.,* 2003; Molyneaux *et al.,* 2003; Stebler *et al.,* 2004; Herpin *et al.,* 2008). In mice, PGCs migration in *SDF-1*-null (Ara *et al.,* 2003) and *CXCR4*-null embryos were examined (Molyneaux *et al.,* 2003). Their analysis revealed that SDF-1/CXCR4 interaction is specifically required for the colonization of gonads by PGCs and survival, but not for earlier stages in PGCs migration. In contrary, Tanaka *et al.* (2005) proposed the unique model of “homing and repulsion” mediated by *Ifitm* genes in PGCs/mesoderm, showing that *Ifitm1* in mesoderm acts as a repulsive guidance cue for *Ifitm3*-positive/*Ifitm1*-negative PGCs into the *Ifitm*-free endoderm. However, the recent genetic analysis by the targeted disruption of the entire *Ifitm* locus clearly showed no detectable influences on migration and development of the germ cell line in the mouse embryos lacking all *Ifitm* genes (Lange *et al.,* 2008), suggesting a minor contribution of a *Ifitm*-mediated guidance for the PGCs migration path into the hindgut endoderm. Therefore, it remains unclear the molecular and cellular mechanisms how PGCs migrate into the hindgut endoderm in mouse embryogenesis.

It was previously shown that migrating PGCs within the hindgut endoderm have initiated a genome-wide epigenetic reprogramming, in addition to alteration in the gene expression (Nakamuta and Kobayashi, 2004; Kurimoto *et al.*, 2008; Sasaki and Matsui, 2008). They undergo a significant loss of both DNA methylation and diMeH3K9, two repressive modifications with higher stability, from their genome at

around 8.0 dpc and instead acquire high levels of triMeH3K27 at around 8.5 dpc (Seki *et al.,* 2005; 2007; Sasaki and Matsui, 2008; Fig. 1-3). Until now, it has remained to be unclear whether the reprogramming in migrating PGCs is cell-autonomous or they are an induced response to their environment, the embryonic hindgut endoderm. Although the developmental potency of PGCs is restricted to the germ lineage, reprogrammed migrating PGCs can acquire pluripotency, as verified by the *in vitro* establishment of pluripotent stem cells and the *in vivo* production of tumors. When PGCs are cultured in the presence of leukemia inhibitory factor (LIF), stem cell factor (SCF) and basic fibroblast growth factor (bFGF), they give rise to embryonic germ (EG) cells (Matsui *et al.,* 1992; Resnick *et al.,* 1992; Fig. 1-3). In addition, germ cell tumors, called teratomas, contain a range of differentiated cell types, including more than two germ layers and embryonal carcinoma (EC) cells. The tumors have been shown experimentally to originate from PGCs (Stevens, 1967; Fig. 1-3). Taken together, PGCs migration and differentiation which occur within the embryonic bodies are risky phenomena, and therefore PGCs behaviors may be regulated strictly in embryogenensis.

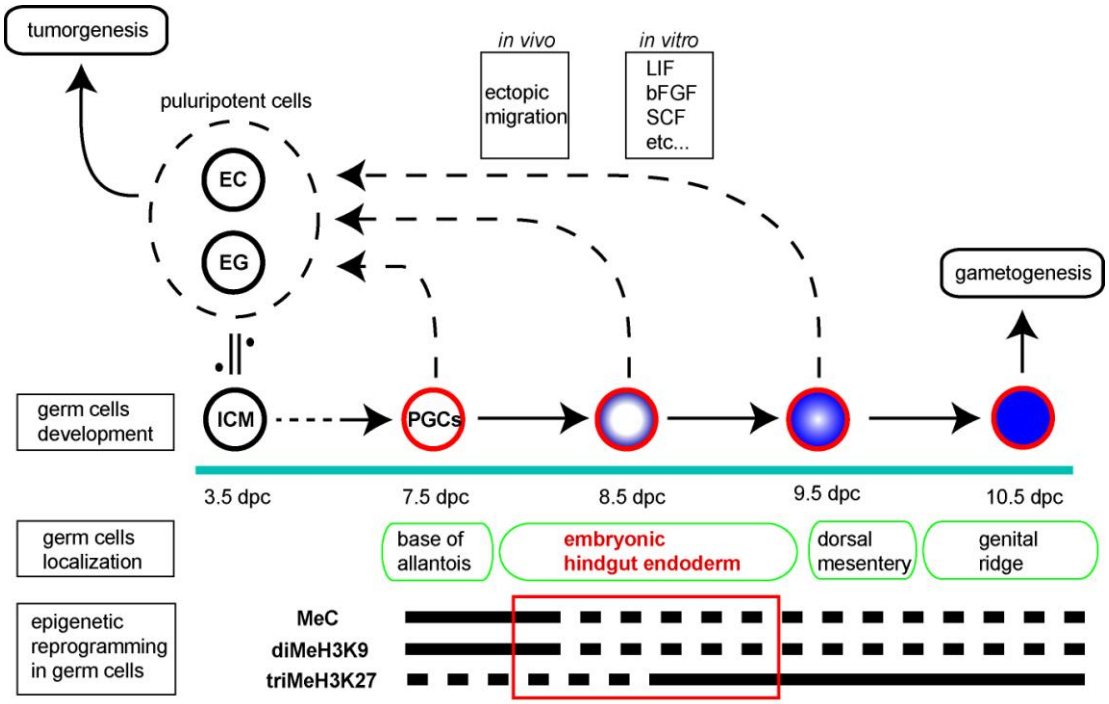

Figure 1-3. **Dynamic epigenetic reprogrammings in migrating PGCs within the embryonic hindgut endoderm.** PGCs undergo a significant loss of both DNA methylation and diMeH3K9, and instead acquire high levels of triMeH3K27 at around 8.5 dpc (indicated by red box). Although the developmental potency of PGCs is restricted to the germ lineage, migrating PGCs which are on the way to reprogramming can acquire pluripotency (e.g. EC (*in vivo*) and EG (*in vitro*)). MeC, 5-methyl cytosine (the product of DNA methylation); EC, embryonal carcinoma cells; EG, embryonic germ cells; ICM, inner cell mass.

The PGCs migration route via the endodermal tissues is widely conserved in various vertebrate and invertebrate species (gut endoderm in nematodes (*C. elegans*) (Sulston *et al.,* 1983); midgut in flies (*Drosophila*) (Warrior, 1994); endoderm in frogs (*Rana pipiens, Xenopus laevis*) (Whitington and Dixon, 1975; Subtelny and Pankala, 1984); hindgut in mice (*mus musculus*) (Moleneaux and Wylie, 2004)), suggesting a potential role of endodermal tissues in the PGCs migration and differentiation during early migratory stages. Therefore, I hypothesized that the embryonic hindgut endoderm is a “key-environment” for PGCs to migrate and differentiate properly during gastrulation in mouse.

The purpose of this study is to clarify the possible roles of the embryonic hindgut endoderm in PGCs migration and differentiation during gastrulation in mouse. In chapter Ⅰ, I examined spatiotemporal relationships between PGCs migration and hindgut formation. In chapter Ⅱ, to examine the significance of embryonic hindgut endoderm environment in PGCs migration and differentiation, I analyzed PGCs behaviors under defective hindgut formation using *Sox17* mutant mouse (Kanai-Azuma *et al.,* 2002). Because, it is now well-established that *Sox17* is crucial for the embryonic hindgut endoderm formation (Kanai-Azuma *et al.,* 2002; Tam *et al.,* 2003). From these analyses, I propose that crucial roles for the embryonic hindgut endoderm in PGCs behaviors during mouse embryogenesis.

2. Chapter Ⅰ
Timing of Primordial Germ Cells Migration and Hindgut Formation

1. Introduction

Precursors of PGCs are staying in the extraembryonic region of the posterior part of the embryo during their specification to PGCs (Anderson *et al.*, 2000; Molyneaux and Wylie, 2004). Shortly after specification, PGCs move through the posterior primitive streak and invade the embryonic hindgut endoderm (Anderson *et al.*, 2000; this study). PGCs keep staying within the newly-formed embryonic hindgut endoderm until 9.5 dpc, and then they migrate toward their target, GRs. Previous studies reported that 8.0 dpc PGCs were round cells with occasional small pseudopodial projections (Clark and Eddy, 1975 Anderson *et al.*, 2000). This indicates non-motile behavior of PGCs themselves at this period. However, these studies were focused on only to PGCs behaviors. In fact, at late gastrulating stage, embryonic mesoderm, embryonic endoderm and extraembryonic mesoderm cells migrate through the primitive streak and differentiate to the component of the posterior part of embryo (Tam and Beddington, 1987; Lawson *et al.,* 1991). These complex morphogenetic movements of the embryo between 7.5 and 8.5 dpc have made it difficult to investigate interactions between PGCs behavior and endoderm morphogenesis during gastrulation. Until now, precise spatiotemporal behaviors of both PGCs and endoderm cells have not been reported.

In this chapter, to clarify a relationship between the endoderm and PGCs regionalization, I first define the timing and entry site of the PGCs movement into the endoderm layer. Next, I show the spatiotemporal correrations between PGCs

migration and hindgut formation during gastrulation.

2. Materials and Methods

All chemicals used in this study were purchased from Wako purechemicals (Japan) unless indicated.

Oct4-EGFP mice

Embryos were obtained from female mice of the outbred strain ICR (SLC, Japan) that were mated with TgN (deGFP) 18Imeg (Oct4-EGFP) heterozygous male mice (Ohbo *et al.,* 2003) maintained in the C57Bl/6 background. All animal experiments were conducted in accordance with the Guidances for Animal Use and Experimentation as set out by the University of Tokyo.

Horseradish peroxidase (HRP)/ALP double staining for visualizing extraembryonic visceral endoderm and PGCs

Embryos were dissected at 7.75~8.0 dpc and incubated in Dulbecco's modified Eagle medium (DMEM; Invitrogen, USA) containing BSA (2.5 mg/ml; Sigma, USA) and horseradish peroxidase (HRP; 1 mg/ml; Sigma) for 1 h. After separation of the head region for genome typing, the embryos were fixed and developed by DAB (Dojindo, Japan) reaction. HRP stained embryos were stained for ALP without dehydration (permeabilization) step. In brief, HRP labeled embryos were washed with ALP-buffer (100mM Tris HCl (pH9.5), 50mM $MgCl_2$, and 100mM NaCl in distilled water (DW)) /0.1% (v/v) Tween20 for 30 min at 4°C. They were then stained with BCIP-NBT (Roche) in ALP-buffer at 4°C. The HRP/ALP double stained embryos

were slightly flattened in 70% (v/v) glycerol under a cover glass. The clearly identifiable purple ALP signals containing a cytoplasmic spot (ALP strong positive) were counted as PGCs located in the endoderm layer, and weak signals were counted as PGCs located just beneath the endoderm layer. I determined the total number of the strong ALP positive PGCs as PGCs stage during late bud to early somite stages (as described in Fig. 2-1 and Fig. 2-3).

DiI labeling and Whole-embryo culture

Embryos at early headfold stage (7.75 dpc) were used for experiments to investigate embryonic endoderm movement. DiI (Carbocyanine fluorescent dye) solution (0.83 μg/ml; Invitrogen, USA) was dripped onto embryos using a micropipette. About 2~3 sec after DiI addition, embryos were rinsed in DMEM to wash out the excess dye. Embryos were cultured in medium containing DMEM supplemented with 75% (v/v) heat-inactivated rat serum for 12~24 h at 37 °C under a humidified atmosphere of 5% CO_2 in a bottle rotating at 30 rpm (Sturm and Tam, 1993). Embryos were examined with a compound fluorescence microscope (Olympus SZX-16).

3. Results

Timing and entry site of the PGCs movement into the endoderm layer at gastrulation stages

First, in order to confirm the timing and entry site of the PGCs movement into the endoderm layer, I isolated whole embryos at the late bud (LB) to early somite stages (7.5~8.0 dpc), incubated them with HRP for the uptake activity of extraembryonic visceral endoderm (Bielinska *et al.,* 1999), and then examined by whole-mount HRP/ALP double staining without permiabilization step. This procedure could allow visualizing both the HRP labeled visceral endoderm (brown staining) and the ALP positive PGCs located within the endoderm (strong purple staining containing cytoplasmic spot, Fig. 2-1B-F) and just beneath the endoderm layer (weak staining, Fig. 2-1B-F) at the posterior proximal region of the mouse embryos. In this staining condition, no ALP-positive reactions are detected in the PGCs located at the allantois region, which is confirmed by frozen section analysis (figure not shown). As shown in Fig. 2-1A, B, a small population of PGCs was first detected in the PGCs entry site located in the HRP-positive extraembryonic visceral endoderm at the base of allantois. Thereafter, the strong ALP-positive population appeared to be increased in number (approximatelly up to 30 PGCs; Fig. 2-1B-G) and migrated along the lateral hindgut region just near the extraembryonic area (Fig. 2-1E, F), while a weak ALP-positive population of PGCs was constantly found in the central PGCs entry site (Fig. 2-1C-E). Analysis of the sectioning samples or the planer samples of the posterior embryonic parts (pressed by cover glass) also confirmed that weak

ALP-positive PGCs were located immediately beneath or near the hindgut endoderm area, suggesting a very restricted entrance of PGCs into the endoderm layer in mouse embryogenesis. Although a quite small population of PGCs (0.64±0.19 PGCs per embryo; n=58) was sometimes located in the HRP-positive visceral endoderm area during gastrulation (open arrows in Fig. 2-1F upper), most of strong ALP-positive PGCs were detected in HRP-negative embryonic endoderm region (Fig. 2-1F). The number of ALP strong positive PGCs was increased, while that of weak positive PGCs was decreased, until S4 stage, indicating that almost all of PGCs population invade the most outer layer of the endoderm before S4 stage (Fig. 2-1G). Finally, most of the PGCs were observed to be located in the hindgut walls by S5 stage (data not shown).

Timings of PGCs migration along the hindgut and the hindgut formation

Next, I examined the spatiotemporal timing of PGCs migration and hindgut formation by using the DiI labeling method to the Oct4-EGFP embryo during 7.75 and 8.5 dpc. As shown in Fig. 2-2A, I labeled putative embryonic hindgut endoderm cells, which were localized in the PGCs entry site, in the early headfold (EHF) stage Oct4-EGFP embryo. After cultured for 12 and 24 h, I examined the localization of PGCs and DiI positive putative endoderm cells localization. As shown in Fig. 2-2B and C, the population of PGCs and DiI positive cells expanded and finally lined along

the hindgut (Fig. 2-2D). Section analysis of 24h cultured embryo clearly revealed PGCs and DiI labeled emnryonic hindgut endoderm were co-localized in the ventral side of the hindgut (Fig. 2-2 E). These results strongly suggest that PGCs and surrounding embryonic hindgut endoderm in the PGCs entry site migrate together along the posterior-anterior axis of the hindgut during hindgut formation.

4. Discussion

Emergence of PGCs and embryonic hindgut endoderm cells at the "PGCs entry site"

Previous observation concerning PGCs migration was focused on PGCs behavior during gastrulation (Anderson *et al.,* 2000). Therefore, it is unclear whether the entrance region of PGCs is extraembryonic visceral or embryonic endoderm area. In this study, I clearly showed that the PGCs entry site is the border between the extraembryonic visceral and embryonic endoderm areas, and almost all PGCs are finally localized within the embryonic hindgut endoderm until 4 somites (S4) stage. In this study, I classify the embryos during LB to early somite stages by the total number of ALP strong positive cells containing cytoplasmic spot in each embryo as "PGCs stage" (Fig. 2-3).

As shown in Fig. 2-1F, after almost all PGCs (approximately 30 in number) invade the embryonic endoderm, HRP negative endoderm cells were observed in the center of "PGCs entry site" (double headed arrow in Fig. 2-3). Recently, surprising data showed that the visceral endoderm cells could contribute to the embryonic hindgut endoderm cells (Kwon *et al.,* 2008). It was disproved the previous common theory, which was the visceral endoderm cells could contribute only to extraembryonic yolk sac endoderm cells. Together with this surprising report, it could consider that composition of the embryonic hindgut endoderm cells in the PGCs entry site derives not only from the newly-supplied embryonic hindgut endoderm

cells through the primitive streak, but also from the characteristically changed visceral endoderm cells. HRP incorporation indicates the characteristic of the visceral endoderm which has many vacuoles in the apical side of epithelial cells. Therefore, HRP non-labeled area indicates embryonic endoderm cells which are derived from two distinct origins. Nevertheless, it was reported that the recruitment of embryonic endodedrm cells from epiblast via the primitive streak to the endoderm continues until the early somite stage (Wilson and Beddington, 1996; Tam *et al*., 2007). These observations suggest that the majority of the embryonic hindgut endoderm cells (red region in Fig. 2-3) are newly-supplied endoderm cells through the primitive streak at the PGCs entry site (gray arrows in Fig. 2-3).

Morphogenetic expansion of the embryonic hindgut endoderm emerged form the "PGCs entry site" and PGCs movement

Next, I focused on the movement of PGCs and the morphogenetic movement of the embryonic endoderm in the PGCs entry site. Interestingly, the mapping study revealed that the endoderm cells in the PGCs entry site expand laterally and strech along the ventral side of the hindgut, which is overlapping PGCs movement, during 7.75 and 8.5 dpc (Fig. 2-2B-D). The pattern of expansion of embryonic hindgut endoderm region (non HRP labeled area) and the regionalization of the PGCs fate imply that cell movement of newly-supplied embryonic endoderm cells and PGCs may be associated with the continuous accretion of cells through the primitive streak

to the surface of embryo until S4 stage (gray arrows in Fig. 2-3), and then PGCs may move by the force of the hindgut endoderm expansion. Previous studies reported that 8.0 dpc PGCs exhibited non-motile behavior at this period (Clark and Eddy, 1975 Anderson *et al.,* 2000). Concomitant with this, it could be considered that PGCs migrate passively with the embryonic hindgut endoderm movement duringlate gastrulation.

5. Figures

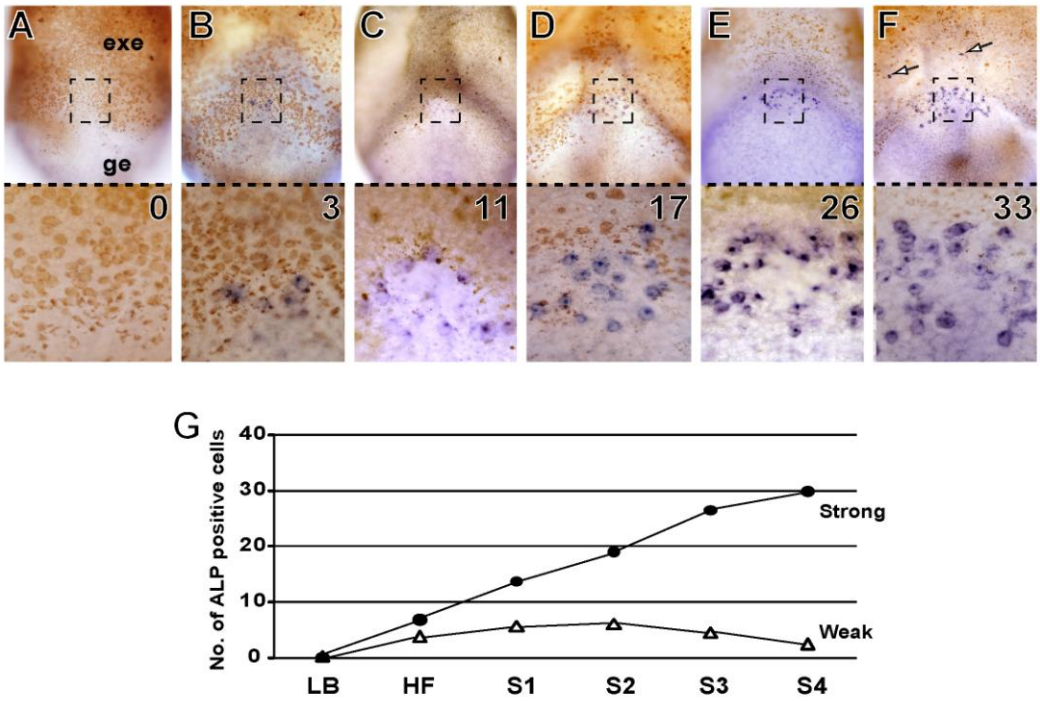

Figure 2-1. **Timing of PGCs movement into the embryonic endoderm**

(A-F) Whole-mount HRP/ALP double staining for showing PGCs located into endoderm layer and embryonic gut endoderm (non-HRP labeled area) during late bud (LB) to early somite stages. Lower panels indicate higher magnification of PGCs entry site in upper panels. Numbers in lower panels indicate total number of ALP strong positive cells containing cytoplasmic spot in each embryo (determined as "PGCs stage" in Fig. 2-3). Open arrows in F show ectopic PGCs migrated away in yolk sac visceral endoderm. (G) Number of PGCs located into endoderm layer by counting ALP positive cells at LB, headfold (HF), 1 somite (S1), S2, S3, and S4 stages (7.5~8.0 dpc; Strong ALP positive, ● ; Weak ALP positive, △). exe, extraembryonic endoderm; ge embryonic gut endoderm.

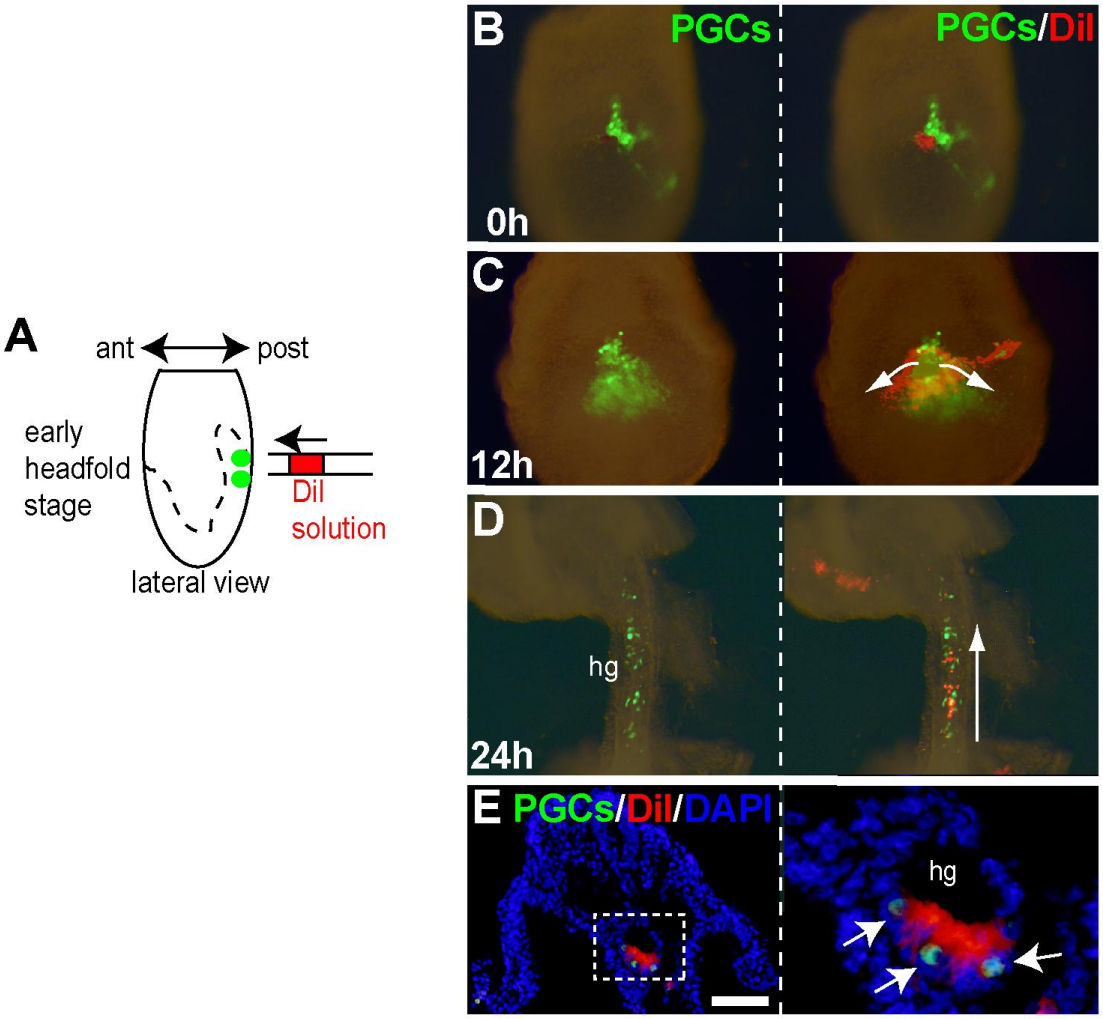

Figure 2-2. **Time course imaging of the morphogenetic expansion of the most proximal posterior endoderm and PGCs migration along the hindgut**

(A) Posterior-proximal endoderm cells in the PGCs entry site of the EHF stage Oct4-EGFP embryo were labeled using DiI solution. (B-E) Spatiotemporal timings of PGCs (green) and DiI labeled endoderm cells (red) movement during hindgut formation. After 12 h culture, PGCs migration path and DiI positive endoderm cells expansion were overlapped (C). After 24 h culture, dissected hindgut portal showing both PGCs and DiI positive cells localized along the posterior-anterior axis of the

hindgut (D). (E) Cryosection of posterior part of embryo cultured for 24 h, with DAPI staining. Right panel in E shows higher magnification of the hindgut in left panel. PGCs and DiI positive endoderm cells co-localized in the ventral side of the hindgut. Arrows indicate PGCs (E, right). hg, hindgut. Bar is 100μm.

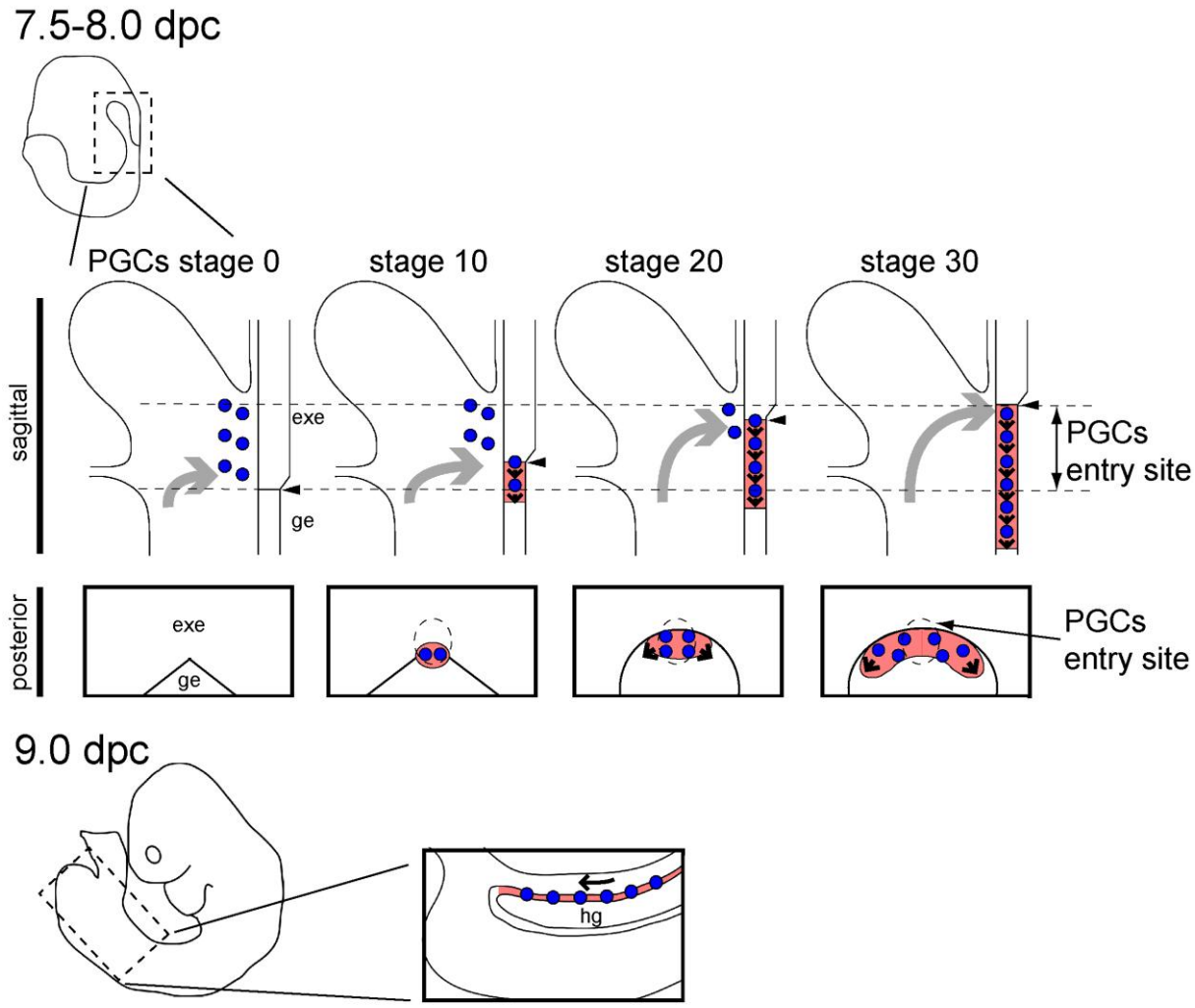

Figure 2-3. **The overlapping pattern of PGCs and newly-supplied embryonic hindgut endoderm cells expansion during late gastrulation**

The PGCs (blue) and the newly-supplied embryonic hindgut endoderm cells (red) emerge at the “PGCs entry site” and migrate together along the hindgut during late gastrulation. Black arrows indicate the overlapping patterns of PGCs movement and embryonic hindgut endoderm expansion. PGCs stages indicate number of PGCs located into endoderm layer. Gray arrows indicate the recruitment of embryonic hindgut endodedrm cells from epiblast via the primitive streak. Black arrowheads indicate the border between the extraembryonic endoderm and the embryonic gut

endoderm. exe, extraembryonic endoderm; ge embryonic gut endoderm; hg, hindgut.

3. Chapter Ⅱ
Crucial Roles of Hindgut Expansion in Directing Proper Migration of Primordial Germ Cells

1. Introduction

In chapter Ⅰ, I showed the similar spatiotemporal correration between PGCs migration and the embryonic hindgut endoderm expansion. This co-regionalization during the gastrulation stages possibly suggests a supportive function of the embryonic hindgut endoderm in PGCs migration and differentiation. To elucidate this, I planned a loss of function analysis of the embryonic hindgut endoderm for PGCs migration and differentiation.

It is now well-established that *Sox17* is crucial for the embryonic endoderm formation in vertebrates (Kanai-Azuma *et al.,* 2002; Tam *et al.,* 2003). The *Sry*-related HMG box gene, *Sox17*, belongs to the Sox subgroup F with *Sox7* (Taniguchi *et al.*, 1999) and *Sox18* (Dunn *et al.,* 1995). Sox17 was originally identified as a stage-specific transcription activator during mouse spermatogenesis (Kanai *et al.,* 1996). Previous study revealed that *Sox17* is specifically activated in endoderm lineage during early gastrulation, and its activity is specifically required for the gut endoderm expansion (Kanai-Azuma *et al.*, 2002; this study). Since *Sox17*-null embryos display the failure of hindgut expansion without any appreciable defects in other tissues by early somites stage (Kanai-Azuma *et al.*, 2002), this mutant embryo is a useful mouse model for the reserchs on the potential inductive/supportive functions of hindgut endoderm in mouse early embryogenesis.

In the present study, I have examined the influence of the specific loss of hindgut

endoderm for PGCs migration and differentiation by using *Sox17*-null embryos and the *Sox17*-null<->wildtype chimeric embryos at early embryogenesis, in order to clarify the endodermal roles in PGCs migration and differentiation. Here, I provide the direct evidence showing that hindgut endoderm expansion is essential for directing proper PGCs migration, not epigenetic differentiation during late gastrulation to early somite stages. These results also imply that defective hindgut endoderm expansion at the PGCs entry site promotes ectopic PGCs migration into yolk sac visceral endoderm, highlighting the importance of the continuous supply and expansion of hindgut endodermal cells for the selection of the PGCs into the correct path to the GRs.

2. Materials and Methods

All chemicals used in this study were purchased from Wako purechemicals (Japan) unless indicated.

Sox17 mutant mice

Embryos were obtained from *Sox17* heterozygous female mice that were mated with *Sox17* heterozygous male mice of the outbred strain ICR. Genomic DNA of the tail tip of mice was isolated using a Wizard genomic DNA purification kit (Promega, USA). For embryonic DNA, a part of the head was dissected from each embryo, and genomic DNA was prepared using the same kit. To analyze the genotype of the embryo by PCR as described below (Kanai-Azuma *et al.,* 2002). All animal experiments were conducted in accordance with the Guidances for Animal Use and Experimentation as set out by the University of Tokyo.

Sox17 wild -allele［235bp］/ *Sox17* mutant -allele［275bp］

Sox17 wt forward

5’- CTC TGC CCT GCC GGG ATG GCA CGG AAT CC -3’

Sox17 wt reverse

5’- AAT GTC GGG GTA GTT GCA ATA GTA GAC CGC TGA -3’

Sox17 mut reverse（pgk promoter）

5’- GCA GGG GCC CTC GAT ATC AAG CTT GGC TG -3’

PCR condition

	95°C	5 min	
Denature	95°C	30 sec	35 cycles
Annealing	58°C	30 sec	
Extension	72°C	30 sec	
	72°C	7 min	

HRP/ALP double staining

I demonstrated HRP/ALP staining as described in M&M of chapter Ⅰ.

ALP staining for detecting and counting PGCs

To count ALP-positive PGC number, embryos up to S6 (6 somite stage) were left intact and embryos over S7 stage were transected into an anterior and posterior portion. The posterior portions of these embryos were split longitudinally along the line of the dorsal aorta. All fragments of the embryos were fixed with 4% PFA-PBS for 6 h at 4°C, and then washed in PBS. For detecting all PGCs, embryos were dehydrated in 70% (v/v) ethanol at 4°C. Then embryos were washed with ALP-buffer /0.1% (v/v) Tween20 for 30 min at 4°C. They were then stained with BCIP-NBT in ALP-buffer at 4°C. The stained pieces from the posterior portion of the embryo were flattened in 70% (v/v) glycerol under a coverslip and the PGCs counted using a compound microscope.

Whole-mount *in situ* hybridization

Whole-mount *in situ* hybridization was performed as previously described by Kanai-Azuma *et al.* (1999). In short, the embryos were fixed in 4% PFA-PBS for 6 h and then dehydrated in methanol. The samples were rehydrated, pretreated with 10μg/ml proteinase K (Merck, USA) in PBST for 3 min, and then hybridized with DIG-labeled *Ifitm3* (*fragilis, mil-1*) RNA probe (kindly provided by Dr. SS. Tanaka, University of Kumamoto, Japan) in a solution containing 50% (v/v) formamide (Invitrogen), 10% (v/v) dextran sulfate (Sigma), 5x SSC, 1% SDS, 50 μg/ml heparin (Sigma) and 50 μg/ml denatured yeast tRNA (Roche) for 36 h at 60^{o}C. After treatment with 100 μg/ml RNase A (Sigma) for 15 min at 37^{o}C, they were washed twice with 5x SSC for 1 h at 65^{o}C. The signals were detected by an immunological method using ALP-conjugated anti-DIG antibody, and NBT and BCIP.

Whole-mount immunohistochemistry

Immunostaining of whole embryos were performed as previously described (Ciruna and Rossant, 2001). In short, embryos were fixed in 4% PFA-PBS for 6 h, then washed in TBST, and incubated with anti-PGC7 Ab (1/10000 dilution; kindly provided by Dr. Y. Matsui, University of Tohoku, Japan) for 12 h at 4°C. After washing with TBST for 1 h three times, they were incubated with Alexa-488 conjugated anti-rabbit IgG Ab (1/200 dilution; Invitrogen, USA) used for 12 h at 4°C, and examined with a compound fluorescence microscope (Olympus SZX-16).

Section immunohistochemistry

Embryos and cultured explants were fixed in 4% PFA-PBS for 12 h at 4°C, dehydrated, and then embedded in paraffin (Fisher scientific, UK). Deparaffinized sections were subjected to ALP staining for PGCs detection using HNPP Fluorescent Detection Set (Roche). For immunohistochemistry, we used anti-SOX17 (1/100 dilution), anti-E-cadherin (1/250 dilition; BD-Pharmingen, USA), anti-diMeH3K9 (1/500 dilution; Upstate, USA), anti-triMeH3K27 Ab (1/500 dilution; Upstate), anti-Metylated Cytosine Ab (1/250 dilution; Calbiochem, USA), anti-p63 Ab (1/50 dilution; Santa Cruz, USA) and anti-PGC7 Ab (1/1000 dilution). The ALP stained sections were incubated with each primary antibody for 12 h at 4°C. Thereafter, the immunoreaction with each first antibody was visualized by Alexa-488 conjugated anti-rabbit IgG Ab (1/400 dilution) or Alexa-488 conjugated anti-mouse IgG Ab (1/400 dilution, Invitrogen) for immunofluorescent, or biotin conjugated anti-rabbit IgG Ab (1/400 dilution; DAKO, Denmark) biotin conjugated anti-rabbit IgG Ab or biotin conjugated anti-mouse IgG Ab (1/400 dilution; Vector) with an ABC Signal Amplification kit (Vector, UK).

Transmission Electron Microscopy

Isolated embryos were fixed in 2.5% (v/v) glutaraldehyde (Nisshin EM, Japan)/0.1 M PB for 4 h at 4°C. After washing in PBS, they were postfixed in 1% (w/v) OsO_4 (Nisshin EM) in 0.1 M PB for 2 h at 4°C. They were then dehydrated and embedded in araldite M. Semi-thin sections (approximately 1 μm) were cut, stained with 1%

(w/v) toluidine blue and observed by light microscopy. Ultra-thin sections (approximately 70 nm) were collected on collodion-coated grids and examined under a JEOL-1010 transmission electron microscope at 80kV.

DiI labeling and Whole-embryo culture

I demonstrated DiI labeling and whole-embryo culture as described in M&M of chapter Ⅰ.

Generation of chimeras and PGCs detection

Sox17-null mutant ES cells were established previously (Kanai-Azuma *et al.*, 2002), and chimeric embryos were generated by blastocyst injection into CAG-EGFP (wildtype) mice (SLC). Embryos were collected at 9.0 dpc. After photographed under a fluorescence microscope, they were fixed with 4% PFA-PBS for 1 h. After embryos were embedded into OCT compound (Sakura, Japan), transverse frozen sections were prepared for PGCs detection by anti-PGC7 Ab. After photographed and stripped in 0.2 M glycine/0.1% (v/v) Tween-20 (pH2.2) for 1 h, sections were immunostained with anti-Laminin Ab (1/1000 dilution; ICN Pharma, USA) to visualize the basal laminae of the hindgut tube. I counted number of PGC7 positive PGCs localization (hindgut or extraembryonic yolk sac) in sections of middle part of the one third length of the hindgut (approximately 300μm). In addition, I also counted whether these PGCs were EGFP positive (wildtype) or negative (*Sox17*-null) (see in Table 3-1).

Statistical analysis

The number of PGCs was compared using the nonparametric Mann-Whitney U-test or Student's t-test.

3. Results

Sox17 localization in the PGCs and the embryonic endoderm during gastrulation

It has been reported that *Sox17* is transiently upregulated in PGCs at around 7.25 dpc from single cell gene expression profiling (Yabuta *et al*., 2006). To confirm this at protein level, I demonstrated Sox17 immunohistochemistry with ALP staining. As a result, Sox17 was observed intensely in PGCs localized in the base of allantois at 7.5 dpc (Fig. 3-1A inset) and downregulated in PGCs after invasion the embryonic endoderm at around 8.0 dpc (Fig. 3-1B, C insets).

During gastrulation, *Sox17* was expressed in the embryonic gut endoderm as shown in Kanai-Azuma *et al*. (2002). At 7.5 dpc, Sox17 was localized in the embryonic gut endoderm (Fig. 3-1A arrowheads). Concomitant with the displacement of the embryonic endoderm and hindgut formation, moderate Sox17 localization was observed in the embryonic hindgut endoderm at the posterior part of the gastrulating embryo (Fig. 3-1B, C arrowheads).

Defective expansion of the embryonic endoderm in *Sox17*-null embryos

In order to examine the morphogenetic movement of the embryonic gut endoderm cells by using fluorescent dye DiI, I labeled the presumptive endoderm area including the PGCs entry site (determined in chapter Ⅰ) in the wildtype (+/+) and *Sox17*-null (-/-) embryos at early headfold stage (Fig. 3-2A), and then cultured for 12 h. DiI

labeled endoderm cells, as well as the PGCs, were properly found to move into the lateral area in the wildtype embryos (arrows in Fig. 3-2B left). In contrast, in the *Sox17*-null embryos, DiI-labeled endoderm was defective in the movement into the lateral region, showing their stay in the original DiI-labeled position throughout the culture period (n=5; Fig. 3-2B right). This is in contrast that the contaminated DiI-labeled extraembryonic visceral endoderm properly expanded into the distal extraembryonic area in the *Sox17*-null embryo (arrowhead in Fig. 3-2B). Such a failure of the hindgut expansion was previously shown to be one of the widely-distributed abnormalities of the primitive streak derivatives in the embryos lacking *Mixl1*, the primitive streak gene upstream of *Sox17* (Hart *et al.*, 2002). Moreover, the previous study showed that Sox17 is specifically activated in and required for the gut endoderm by early somite stages (Kanai-Azuma *et al.*, 2002). Therefore, it is likely the *Sox17*-null mutant is a mouse model useful for studying potential roles of hindgut endoderm in PGCs migration and differentiation.

No appreciable defects are detected in the initial specification and colonization of PGCs in *Sox17*-null embryos

Next, I examined whether the PGCs in *Sox17*-null embryos are properly specified and clustered at the base of allantois region or not. At early to late gastrulation, several PGCs marker including *Ifitm3* (Fig. 3-3A), *PGC7* (Fig. 3-4E)*, Nanog* (data not shown)*, Oct4* (data not shown), *ALP* (Fig. 3-3B) and *p63* (Fig. 3-7C) were properly

expressed in the *Sox17*-null PGCs, showing similar to those in the wildtype/heterozygote littermates. Moreover, by using the standard whole-mount ALP staining with permiabilization procedures, the average numbers of ALP positive PGCs at 7.75 dpc (late bud to early headfold stage) were not significantly different in *Sox17*-hetero (+/-, 39.6) and -null (-/-, 32.0) compared with wildtype embryos (+/+, 35.3) (Fig. 3-3C). With regard to proper epigenetic reprogramming and histone modifications of the PGCs at the later stages (Fig. 3-7A, B), this clearly indicates no appreciable defects in their specification and differentiation in the *Sox17*-null mutants throughout gastrulation. Sectioning analysis also confirmed that the most-front PGCs were closely associated with hindgut area (Fig. 3-3D upper), suggesting no appreciable defects in their environment into the entry site of the hindgut layer. Moreover, anti-Laminin immunostaining also revealed that discontinuous basal laminae were found along the area both in wildtype and *Sox17*-null embryos (open arrows in Fig. 3-3D lower), indicating the open state of the PGCs entry site within the posterior embryos. Therefore, I conclude that PGCs were adequately formed in the *Sox17*-null embryos. PGCs formation and migration toward the endoderm layer are independent of the activity of Sox17 in the mouse embryo.

A front population of the PGCs is immobile within the hindgut endoderm throughout the early embryogenesis, but the remaining PGCs ectopically migrate away into the yolk sac endoderm in *Sox17*-null embryos

Next, the timing and movement into the hindgut endoderm were examined in the *Sox17*-null embryos by using whole-mount ALP/HRP double staining without any permeabilization steps. At early headfold stage, 5~10 strong PGCs were properly found to be in the PGCs entry site at the border of the extraembryonic region (Fig. 3-4A), showing similar to those in the wildtype embryos at the same stage. In the wildtype embryos at late headfold stages, the PGCs at the entry site were increased in number, and then moved into the lateral area of the hindgut region. In contrast, in the *Sox17*-null mutants, neither increase of the PGCs number within the entry site nor lateral movement of the PGCs was detected (Fig. 3-4B). Moreover, most interestingly, instead of the increase of the PGCs number in the embryonic endoderm area, the PGCs were frequently found to be ectopically located in the HRP-positive extraembryonic endoderm that were outside of the PGCs entry site after PGCs stage 10 (Fig. 3-4B, C right). At the late headfold stage to early somite stage, the number of ectopic PGCs in the extraembryonic region was clearly increased as compared with those in wildtype embryos at 8.75 dpc (Fig. 3-4B-E right). Such ectopic PGCs in the extraembryonic endoderm appeared to migrate away from the PGCs entry site into the extraembryonic yolk sac endoderm during 8.0 to 9.5 dpc (arrowheads in Fig. 3-4B-F). In contrast, the PGCs within the entry site was continuously detected

throughout the early embryogenesis, showing the remaining PGCs at the entry site in *Sox17*-null site (Fig. 3-4B, C, D, F right), and no PGCs migrated within the hindgut tube (Fig. 3-4F right lower). Therefore, these findings suggest that the hindgut endoderm formation directs proper PGCs migration path not into the extraembryonic visceral endoderm.

To quantitatively examine the PGCs number in the ectopic position, the number of ALP-positive PGCs located in the embryonic/extraembryonic endoderm and allantois regions was separately estimated in each embryo. During 8.25 to 8.75 dpc (0~14 somite stage), approximately 10 PGCs at the entry site of the hindgut were stable in number in the *Sox17*-null (-/-) embryos throughout early somite stages (solid lines in Fig. 3-4G left), in contrast to the increase of the PGCs in the hindgut of the wildtype (+/+) / heterozygous (+/-) embryos (open lines in Fig. 3-4G left). In contrast, the number of the ectopic PGCs in the extraemryonic endoderm was increased in the *Sox17*-null embryos (Fig. 3-4G middle). The average number of PGCs remaining into allantois in the *Sox17*-null (-/-) embryos was not different when compared with wildtype (+/+) or *Sox17*-hetero (+/-) embryos (Fig. 3-4G right).

Tight connection between the PGCs and presumptive endoderm cells at the entrance to the hindgut endoderm in 8.0dpc *Sox17*-null embryos

As described above, the present data indicate that, in the *Sox17*-null embryos, PGCs could properly move into the PGCs entry site into the gut endoderm, but they

were motionless within this region throughout the somite stages (Fig. 3-4A-F right). Since the *Sox17*-null defective endoderm display defective expansion (Fig. 3-2B right), this clearly arises the possibility that the PGCs was trapped by the aberrant expansion of the *Sox17*-null hindgut endoderm cells at the entry site. Next, I examined the expression pattern of E-cadherin, an endoderm marker, around the posterior area including the PGCs entry site (Fig. 3-5A). E-cadherin was moderately expressed in embryonic endoderm of wildtype (+/+) embryos (Fig. 3-5B). Interestingly, in the *Sox17*-null embryos, E-cadherin positive cells aggregated tightly at the entry site into the hidgut endoderm, where several PGCs were included and surrounded by the E-cadherin positive cells (Fig. 3-5C). Ultrastructural analysis also confirmed tight connection of PGCs with surrounding putative hindgut endoderm cells at the most-posterior region in the *Sox17*-null embryo (Fig. 3-5E). Presumptive E-cadherin positive aggregated cells were tightly connected with the most out embryonic endoderm cells in addition to the PGCs (Fig. 3-5E), and these tight connection including adherens junction was continuously found in the cells inside the endoderm layer (arrows in Fig. 3-5E). With regard to these aggregated cells expressing E-cadherin, this suggests that these aggregated cells are presumptive defective embryonic hindgut endoderm cells. This further indicates that defective expansion of the hindgut endoderm likely causes the motionless of the PGCs to the outer layer of the gut region in the *Sox17*-null embryos.

Supply of wildtype endoderm cells can rescue defective migration of the *Sox17*-null PGCs by chimera analysis

From the *Sox17*-null embryo analysis, I postulated that the disruption of PGCs migration was due to defective movement of the embryonic gut endoderm. If this model is correct, specific complementation of the *Sox17*-null embryos with wildtype embryonic endoderm should allow *Sox17*-null embryos to complete PGCs migration along hindgut.

It was previously reported the lack of contribution of *Sox17*-null ES cells in the hindgut endoderm in the chimera (Kanai-Azuma *et al.,* 2002). To assess the impact of the support of functional embryonic endoderm which expresses *Sox17* in PGCs migration, I examined the chimeric embryos comprised of *Sox17*-null ES cells and blastocyst derived from CAG-EGFP (wildtype) mice, which constitutively express EGFP.

I obtained chimeric embryos with the high contribution of *Sox17*-null ES cells (Fig. 3-6C, E) and non-chimeric littermates (Fig. 3-6A) at 9.0 dpc. Two chimeras were provided with various degrees of mutant ES cell contribution. One chimera with high mutant ES cell contribution displayed no axis rotation (Fig. 3-6E), while another chimera containing moderately high mutant ES cell contribution showed late axis rotation (Fig. 3-6C). After each whole-mount embryo was photographed (Fig. 3-6A, C, E), transverse frozen sections were prepared for histological analysis (Fig. 3-6B, D, F, G).

In chimeric embryos, PGCs (PGC7 positive cells) were contributed by *Sox17*-null ES cells (arrows in Fig. 3-6D, F, G). In chimeric embryos, 90.1% (272/302) of PGCs were detected as *Sox17*-null mutant (n=4, Table 3-1). This result shows that Sox17 in PGCs is not necessary for the process of PGCs migration at least before 9.0 dpc.

As shown in middle panels of Fig. 3-6D, F and G, I revealed that *Sox17*-null ES cell-derived PGCs had migrated along the hindgut in chimeric embryos complemented with functional embryonic hindgut endoderm (n=4). In addition, Table 3-1, only 2.3% (7/302) PGCs ectopically migrated toward yolk sac, in constrast to phenotypes of *Sox17*-null mutant. These results strongly support my hypothesis that the aberrant PGCs migration is a resultant of deficiency in embryonic endoderm expansion in the *Sox17*-null embryo. Furthermore, as shown in middle panel of Fig. 3-6G, *Sox17*-null ES cells derived embryonic hindgut endoderm cells which had a contact with PGCs were observed. Therefore, PGCs migration along the hindgut might be supported by non-cell autonomous activity of Sox17 in the embryonic endoderm.

Proper epigenetic reprogramming progression of ectopic PGCs in the extraembryonic endoderm

It was previously shown that a genome-wide dynamic epigenetic reprogramming initiates at the migratory period (Seki *et al.*, 2005; 2007). Moreover, the expression of several PGCs markers is initiated at the hindgut migratory stage (Nakamuta and Kobayashi, 2004; Kurimoto *et al.,* 2008). Finally, I examined the expression patterns of several differentiation markers in the PGCs located in the presumptive embryonic hindgut endoderm and the extraembryonic yolk sac endoderm tissues of the *Sox17*-nll (-/-) and wildtype (+/+) embryos.

The germ-lineage expression of p63, an essential factor to protect the germ

lineage during meiotic arrest (Suh *et al.*, 2006), was shown to be first activated in the PGCs at hindgut stage (Nakamuta and Kobayashi, 2004). In the *Sox17*-null embryos, p63 expression was observed at 8.5 dpc (Fig. 3-7C), and epigenetic DNA and histone modifications (MeC down-regulation, diMeH3K9 down-regulation and triMeH3K27 up-regulation) were also observed adequately during 7.5 and 8.5 dpc in the ectopic PGCs of the *Sox17*-null (-/-) embryos (Fig. 3-7A, B). These results suggest that p63 expression and epigenetic modifications in migrating PGCs are independent of localization within the embryonic endoderm. These differentiations in ectopic PGCs proceed cell-autonomously or are also supported in the yolk sac environment.

4. Discussion

Sox17 mutant is the good model for the research in the inductive/ supportive roles of the gut endoderm in PGCs migration and differentiations at early-headfold to early-somite stages.

The *Sox* gene family shows a high level of amino acid homology in the DNA-binding HMG domain and shares homologous amino acid sequences outside the HMG box domain within the same group (Bowles *et al*., 2000). Moreover, several members are co-expressed in the same cell type and have redundant functions in the same developmental processes (Lefebvre *et al.*, 2007). In mouse embryogenesis, Sox17 is activated in several distinct cell lineages except for embryonic endoderm and its derivatives such as extraembryonic visceral endoderm (Kanai-Azuma *et al.*, 2002; Shimoda *et al.,* 2007), vascular endothelial cells (Matsui *et al.*, 2006; Sakamoto *et al*., 2007; Cermenati *et al.,* 2008), hematopoietic cells (Kim *et al.*, 2007), oligodendrocytes (Shon *et al.,* 2006) and germ cell lineage (Kanai *et al*., 1996; Yabuta *et al.*, 2006; de Jong *et al.,* 2008). Although Sox17 activity has potentially crucial roles in various cell types of mouse embryos, *Sox17*-null embryos show the reduced population of embryonic endoderm and defective expansion of hindgut endoderm, but does not display any appreciable defects in other cell types by early somite stages, except for aberrant heart looping, enlarged cardinal vein and defects in formation of anterior dorsal aorta (Kania-Azuma *et al.*, 2002; Sakamoto *et al.*, 2007). This is likely due to the redundancy of the other Sox members in the cell types except for gut endoderm (Matsui *et al.,* 2006; Sakamoto *et al.*, 2007). Moreover,

chimera analysis allows providing the *Sox17*-null embryos with the specific replacement of the wildtype hindgut endoderm cells (Kanai-Azuma *et al.,* 2002; this study). Therefore, these data clearly imply that the *Sox17* mutant is the good model for the research in the inductive/supportive roles of the embryonic gut endoderm in PGCs migration and differentiation at early headfold to early somite stages.

Crucial function of embryonic hindgut endoderm as "conveyor belt" of the PGCs transport system in mouse embryogenesis

By using *Sox17*-mutant, I here provide the direct evidence for the crucial function of hindgut endoderm as a "conveyor belt" of the PGCs transport system in mouse embryogenesis. In the *Sox17*-null embryo, the PGCs were properly specified and colonized at the base of allantois, and then the front of PGCs population (approximately 10 PGCs) properly moved into the E-cadherin positive presumptive endoderm cells. This PGCs population was trapped within this site and blocked to migrate away into the hindgut endoderm throughout gastrulation. Chimera analysis of *Sox17*-null ES cells showed that only the supply of wildtype endoderm cells can rescue defective PGCs migration in the proper hindgut position. Therefore, my results imply that defective hindgut expansion promotes PGCs migration into the gut area in early mouse embryogenesis.

An approximately 10 PGCs are maintained at the PGCs entry site in the

developing *Sox17*-null embryos, suggesting that the front PGCs are immobile throughout the gastrulation and early somite stage. Moreover, E-cadherin positive presumptive endoderm cells are aggregated and trapped at this region, suggesting that aggregation of these cells is likely due to the defective expansion of hindgut cells into the outer gut endoderm layer, indicating the roles of hindgut endoderm expansion in PGCs movement within embryonic endoderm layer.

Interestingly, the remaining population (15~20 cells) ectopically migrate away into the extraembryonic visceral endoderm through the PGCs entry site at the extraembryonic side. These findings clearly indicate that the defective supply and expansion of embryonic endoderm at the PGCs entry site cause repulsive effects to PGCs. Therefore, the supply and expansion of the embryonic hindgut endoderm at the PGCs entry site are essential for PGCs movement into embryonic body. In other words, the “PGCs entry site” acts strictly as the first gate for the correct path of PGCs movement toward GRs.

Chimeras with high mutant ES cell contribution also failed to undergo axis rotation at 9.0 dpc, which replicates the phenotype of the *Sox17*-null mutant embryos. I previously reported aberrant heart looping, enlarged cardinal vein and defects in formation of anterior dorsal aorta in *Sox17*-null embryos at around 8.5 dpc (Sakamoto and Hara *et al.,* 2007). Although similar defects were also observed in chimeric embryos, PGCs migration along the length of hindgut was rescued by the supply of wildtype embryonic endoderm. Therefore, defects of the axis rotation and

the cardiovascular formation do not affect PGCs migration. These results support the importance of specific interaction between the PGCs and the embryonic hindgut endoderm on PGCs migration along hindgut during 7.75 and 8.5 dpc.

Once PGCs migrate into the embryonic hindgut endoderm, they exhibit a round cell shape and have a contact with the embryonic endoderm in the wildtype embryos (Clark and Eddy, 1975; Anderson *et al.*, 2000). On the other hand, many ectopic PGCs, which localized between the extraembryonic visceral endoderm and the extraembryonic mesoderm, displayed amoeboid in shape in the *Sox17*-null embryo (data not shown). In addition, PGCs obtained from 8.5 dpc embryo exhibit a polarized morphology in clonal *in vitro* culture (Ohkubo *et al.*, 1996). Taken together with these results, PGCs may have an essentially migratory phenotype. It seems that a possible role of the embryonic endoderm is to repress PGCs motility. Interestingly, the large numbers of ectopic PGCs continue to be motile, while all of PGCs become stationary after entrance into gonad at 11.0 dpc (Stallock *et al.,* 2003). These data suggest that contact with specific somatic cells (embryonic endoderm or soma of gonad), rather than an inherent timing mechanism, is required to switch off the migratory phenotype of PGCs.

It was reported that the steel-c-kit interaction is required for PGCs to colonize, survive and migrate within the hindgut (Besmer *et al.*, 1993; Buehr *et al.,* 1993). PGCs in W^e/W^e (the White extreme allele of *c-Kit*) embryos were confined to the ventral side of the hindgut (Buehr *et al.,* 1993). Authors discussed that it was independent of normal *c-kit* expression on PGCs migration along the entire length of

the hindgut. From the present study, PGCs may be transported along the ventral side of the hindgut by the embryonic gut endoderm movement, and then they could not migrate dorsally by the loss of c-kit function in W^e/W^e mutant mice.

Genetic and epigenentic maturation in migrating PGCs is independent of localization within the embryonic endoderm environment.

Many aspects of PGCs phenotype change at about the time of entry into the GRs. Several reports suggested that PGCs have an intrinsic mechanism for the measurement of timing of entry into meiosis (Ohkubo *et al.*, 1996; McLaren and Southee, 1997; Chuma *et al.*, 2001). Donovan *et al.* (1986) suggested that the shift in PGCs behavior and expression of cell surface antigens before and after entry into GRs might be a response to an intrinsic clock that regulates their development, since they behave in culture much as they do in the embryo. The report that addition of 5-azacytidine to the culture medium accelerates the induction of GCNA1 (Maatouk and Resnik, 2003), independently of cell proliferation, raises the possibility that an epigenetic process involving DNA or histone demethylation may play a role in any timing mechanism that regulates PGCs development. Together with these reports, PGCs may have an intrinsic timing mechanism of their differentiation.

My analysis on PGCs also supports this notion concerning p63 expression, DNA demethylation and histone modifications. However, it has left the possibility whether these changes are cell-autonomous or they are an induced response to the

extraembryonic visceral endoderm environment.

In conclusion, the present data provides the direct evidence showing the crucial function of embryonic hindgut endoderm as a “conveyor belt” of the PGCs transport system in mouse embryogenesis. I demonstrate that, in the *Sox17*-null embryos, the front population of the PGCs is trapped and motionless within presumptive endodermal cells at the PGCs entry site, but the remaining PGCs move into the ectopic extraembryonic yolk sac endoderm through the distal entry site of the extraembryonic visceral endoderm during late gastrulation (Fig. 3-8). These data clearly suggest that the continuous supply of the embryonic hindgut endoderm expansion promotes ectopic PGCs migration into yolk sac endoderm, highlighting the importance of the continuous supply and expansion of embryonic endoderm cells for selection of the PGCs progress into the correct path to the GRs. The present study also shows that the PGCs into the proper epigenetic reprogramming in the ectopic PGCs, supporting the hypothesis that the epigenetic maturation and differentiation progress cell-autonomously.

5. Table and Figures

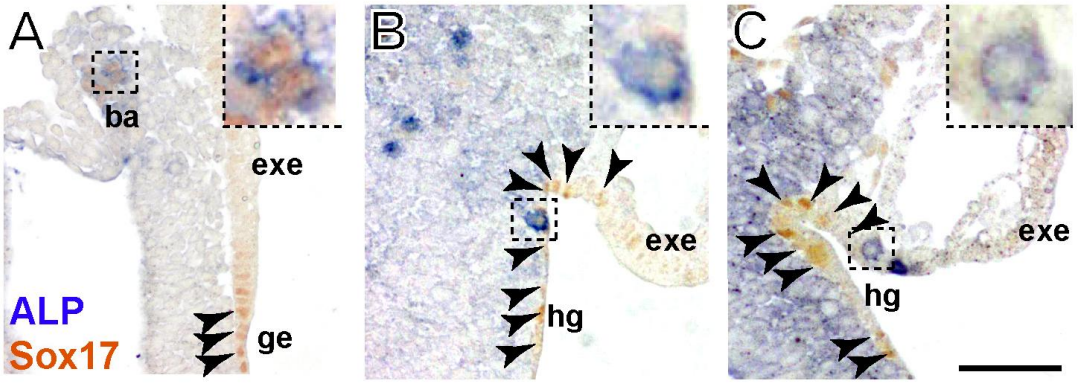

Figure 3-1. **Sox17 localization in the PGCs and the embryonic gut endoderm during hindgut formation in mouse embryo**

(A-C) Sagittal views of posterior parts of late bud (A, 7.5 dpc), late headfold (B, 8.0 dpc) and early somite stage (C, 8.5 dpc) mouse embryos showing the localization of Sox17. Insets of each panel show higher magnified images of ALP positive PGCs. Arrowheads indicate Sox17 localization in the embryonic endoderm. ba, base of allantois; exe, extraembryonic visceral endoderm; ge, embryonic gut endoderm; hg, embryonic hindgut endoderm. Bar is 50μm.

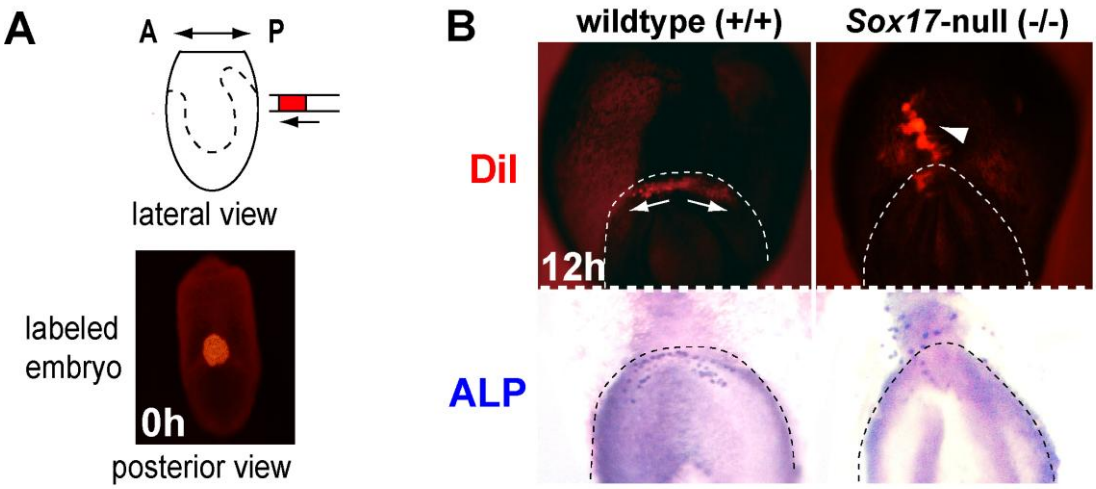

Figure 3-2. **Defective expansion of the embryonic endoderm in *Sox17*-null embryos**

(A) The endoderm cells in PGCs entry site of the early headfold stage embryo were labeled using DiI solution. (B upper) Morphogenetic movements of the early headfold posterior embryonic endoderm during 12 h culture in wildtype (+/+, left upper) and *Sox17*-null embryos (-/-, right upper) show the defective expansion of embryonic endoderm in *Sox17*-null embryo. (B lower) Whole-mount ALP staining in wildtype (+/+, right lower) and *Sox17*-null embryos (-/-, right lower). Arrows in B (left) indicate the direction of embryonic endoderm expansion. Arrowhead in B (right) indicates the proper migration of contaminated extraembryonic endoderm. Dotted lines indicate the border between the embryonic and the extraembryonic endoderm.

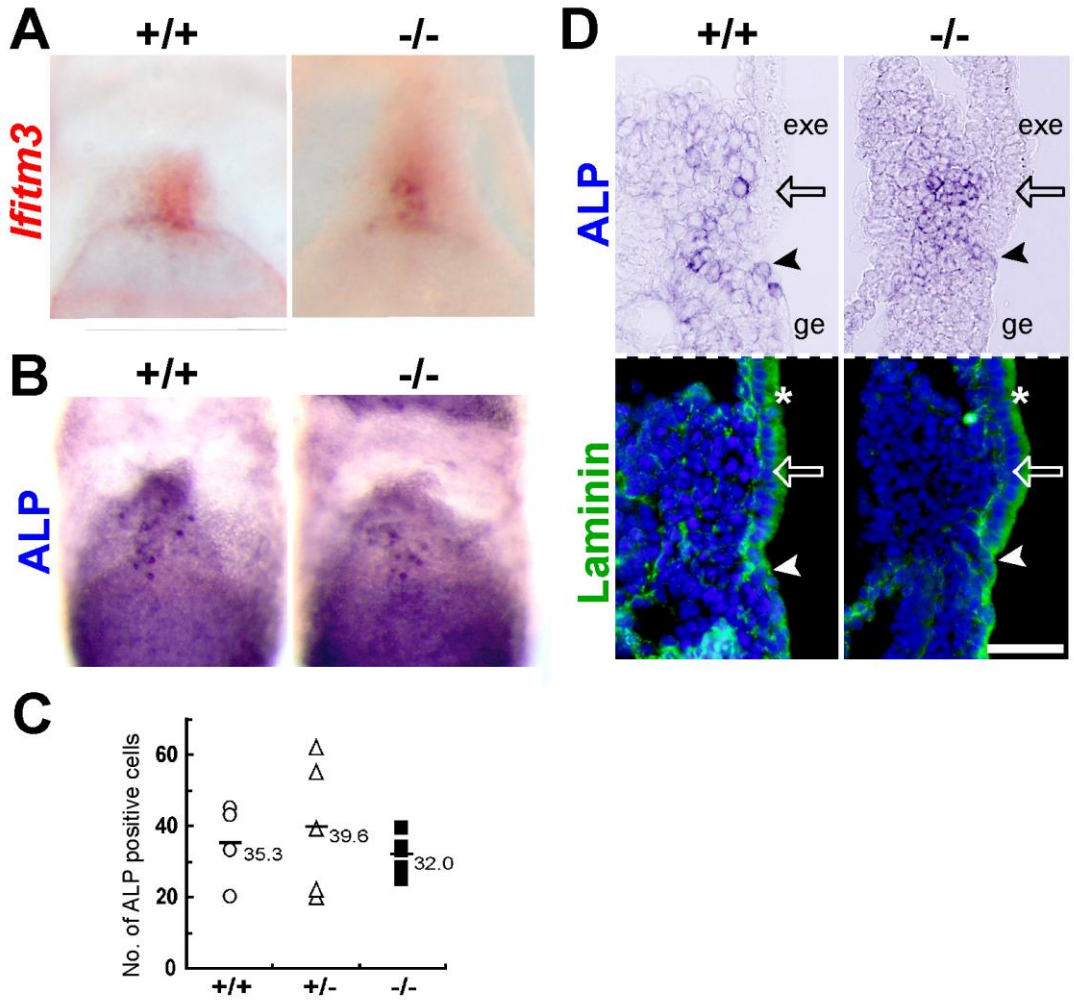

Figure 3-3. **No appreciable defects are detected in the initial specification and colonization of PGCs in *Sox17*-null embryos.**

(A) Expression of *Ifitm3*, a PGCs specific marker, at the base of allantois at early headfold stage wildtype (+/+, left) and *Sox17*-null embryos (-/-, right). (B) Whole-mount the ALP staining in early headfold stage wildtype (+/+, left) and *Sox17*-null embryos (-/-, right). (C) Average number of total ALP-positive PGCs in early headfold stage wildtype (+/+, n= 4), *Sox17*-hetero (+/-, n= 5) and *Sox17*-null embryos (-/-, n= 6). There were not significant differences between wildtype versus *Sox17*-hetero (P = 0.70), and wildtype versus *Sox17*-null embryos (P = 0.54) in PGCs

number. (D) Sagittal sections of posterior proximal regions of early headfold stage wildtype (+/+) and *Sox17*-null embryos (-/-) showing PGCs migration outward from the base of allantois toward the embryonic endoderm of each embryo. Upper panels indicate ALP staining for PGCs (purple). Lower panels indicate Laminin immunostaining with DAPI staining showing the basal membrane (green). Arrowheads indicate the border between the embryonic and the extraembryonic endoderms. exe, extraembryonic endoderm; ge, embryonic gut endoderm. Asterisks indicate background of Laminin immunostaining in the extraembryonic visceral endoderm. Bar is 100μm.

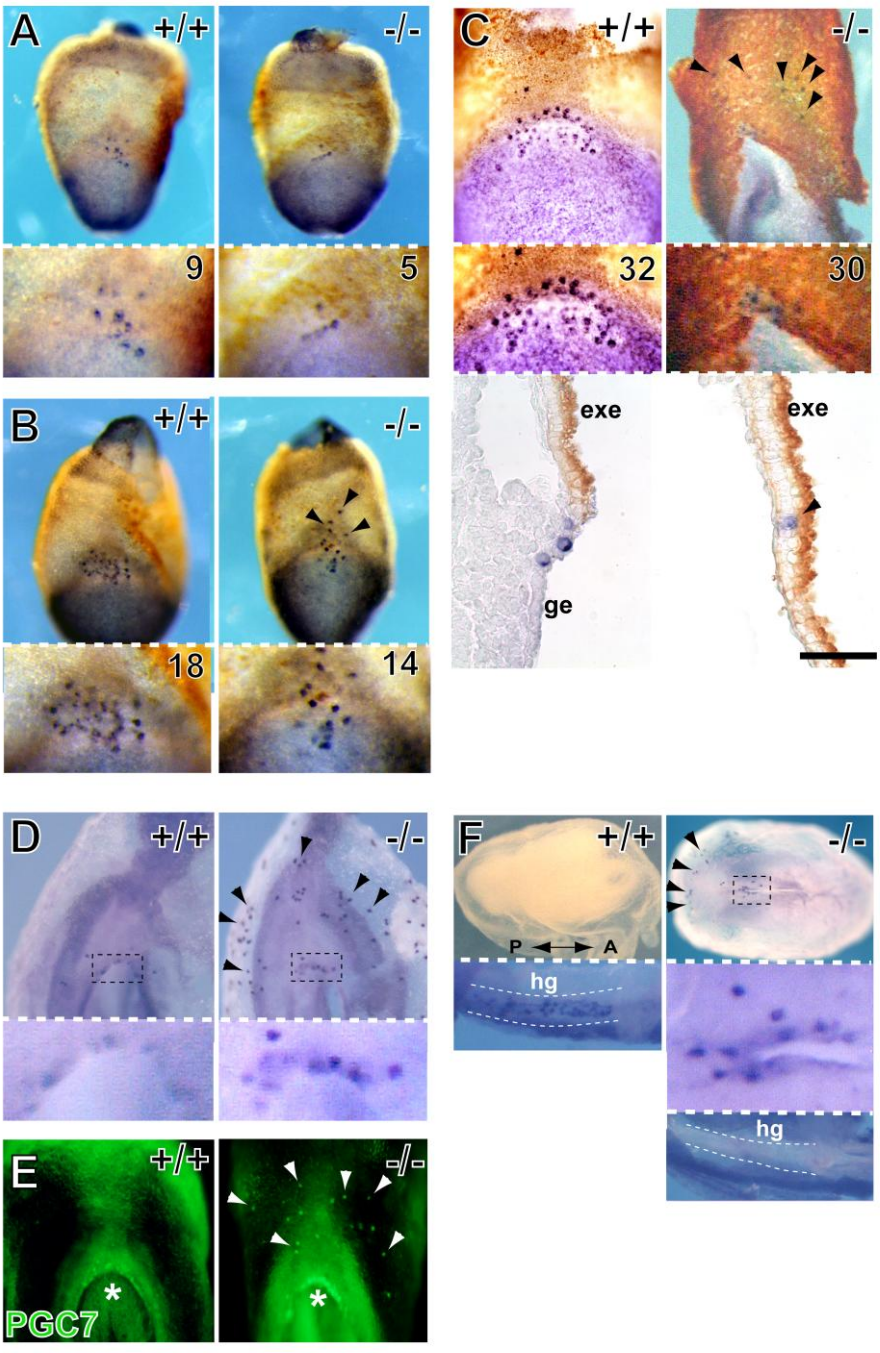
A
+/+
-/-
9
5
B
+/+
-/-
18
14
C
+/+
-/-
32
30
exe
ge
exe
D
+/+
-/-
E
+/+
-/-
PGC7
F
+/+
-/-
P
A
hg
hg
G
gut endoderm
extraembryonic endoderm
allantois
No. of ALP positive cells
+/+ or +/-
-/-
8.25
8.5
8.75

Figure 3-4. **Impaired PGCs migration in *Sox17*-null embryos after 8.0 dpc**

(A-C) Posterior views of whole-mount HRP/ALP double staining in wildtype (+/+) and *Sox17*-null embryos (-/-) at early headfold (A, B) and early somite stage (C) show localization of PGCs (purple staining), extraembryonic visceral endoderm (brown staining) and embryonic endoderm (non-labeling-area). Lower panels of A and B, and middle panel of C indicate PGCs stage as determined in Chapter Ⅰ. Sagittal sections in C are shown on the lower in each plate. Asterisks in C indicate PGCs entry site. Arrowheads indicate ectopic PGCs in the extraembryonic visceral endoderm. exe, extraembryonic endoderm; ge, embryonic gut endoderm. Bar is 100μm. (D, E) Posterior views of whole-mount ALP staining (D) and PGC7 immunostaining (E) in wildtype (+/+) and *Sox17*-null embryos (-/-) at 8.5 dpc. Lower panels in D indicate higher magnification of PGCs entry site of each embryo. Asterisks in E indicate the PGCs entry site (entrance of gut tube). (F) Ventral views of whole-mount ALP staining in wildtype (+/+) and *Sox17*-null embryos (-/-) at 9.5 dpc. Lower panels indicate PGCs localization in the hindgut of each embryo. Middle panel in *Sox17*-null (-/-) embryo indicates PGCs entry site. White dotted lines indicate the hindgut tube. Middle panel of *Sox17*-null embryo indicates higher magnification of immobile PGCs at PGCs entry site. hg, hindgut.

(G) The average numbers of PGCs localized in embryonic or presumptive embryonic endoderm (left), extraembryonic endoderm (center) and allantois (right) at 8.25 (S1-5 stage), 8.5 (S6-10 stage), and 8.75 dpc (S11-15 stage) in wildtype or *Sox17*-hetero (+/-, open lines), and *Sox17*-null embryos (-/-, solid lines), respectively.

Single asterisk, $P<0.05$; double asterisk, $P<0.01$.

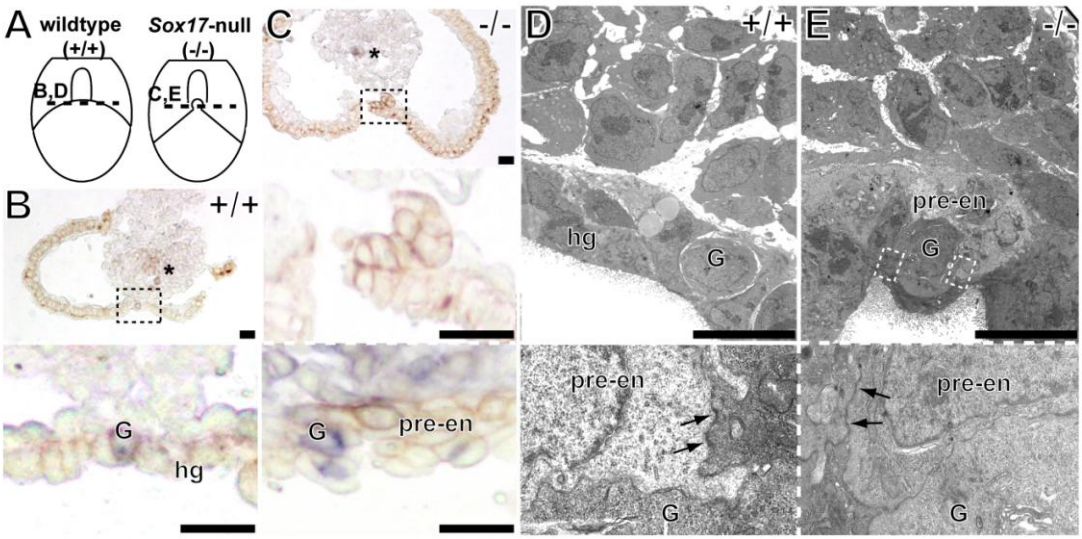

Figure 3-5. **Tight accumulation of PGCs and surrounding presumptive embryonic endoderm cells in 8.0 dpc *Sox17*-null embryos**

(A) Schematic representations of posterior views of wildtype (+/+) and *Sox17*-null embryos (-/-) showing transverse-section areas in B-E. (B, C) ALP staining (purple staining) and E-cadherin immunostaining (brown staining) of 8.0 dpc wildtype (+/+) (B) and *Sox17*-null embryos (-/-) (C). Lower and middle panels in B and C show higher magnified views of each embryo. (D, E) Transmission electron micrographs showing embryonic or presumptive embryonic endoderm cells and PGCs of 8.0 dpc wildtype (+/+, D) and *Sox17*-null embryos (-/-, E). Lower panels in E show higher magnification of PGCs and presumptive embryonic endoderm of *Sox17*-null embryos (-/-). Arrows indicate adherens junctions between the presumptive embryonic endoderm cells and the most out embryonic endoderm cells. hg, embryonic hindgut endoderm; G, PGCs; pre-en, presumptive embryonic endoderm. Bars are 30μm.

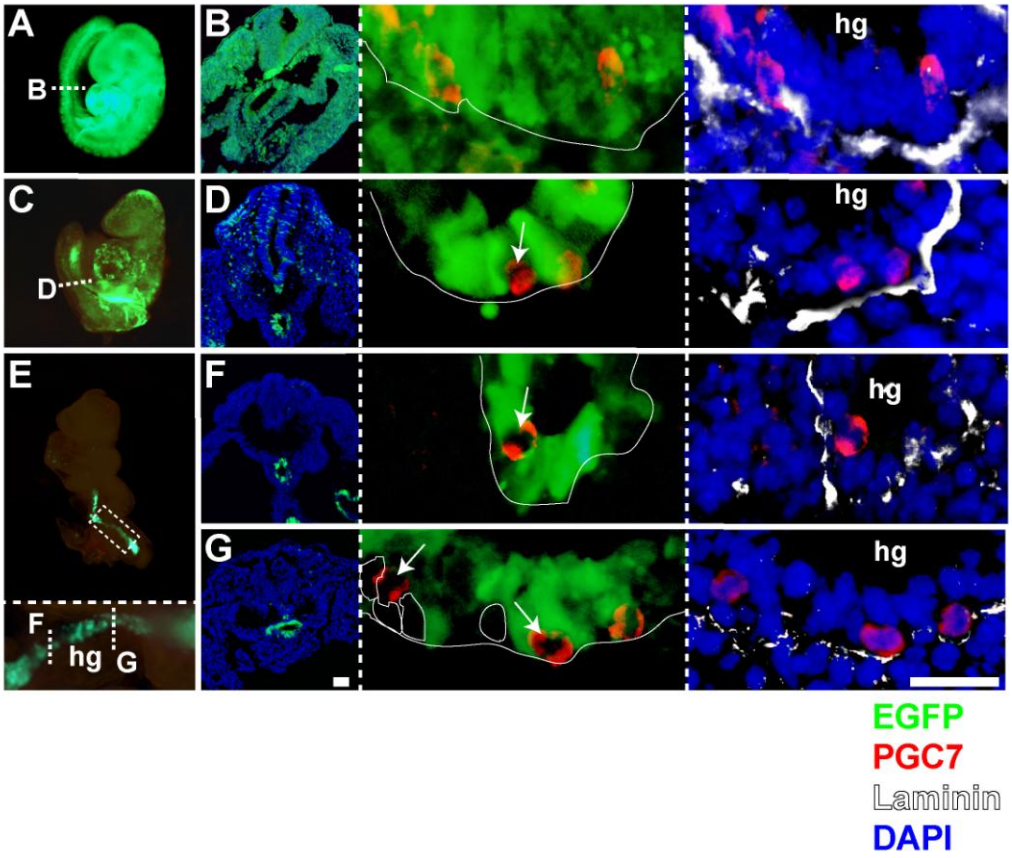

Figure 3-6. ***Sox17*-null ES cell-derived PGCs migrate along the hindgut in chimeric embryos complemented with functional embryonic endoderm**

Chimeric embryos were generated by blastocyst injection of *Sox17*-null (-/-) ES cells (EGFP negative) into CAG-EGFP (wildtype (+/+), green) mice.

(A, C, E) Whole-mount view of chimeric embryos with high contribution of *Sox17*-null ES cells (C, E) and non-chimeric littermates (A) at 9.0 dpc. Two chimeras with various degrees of mutant ES cell contribution: one chimera with high mutant ES cell contribution displayed no axis rotation (E), while other chimera containing moderately high mutant ES cell contribution showed late axis rotation (C). Higher magnification of hindgut region of E is shown in lower panel of E.

(B, D, F, G) Transverse sections of each chimeric embryo at 9.0 dpc with DAPI

staining (left panels). Higher magnification of hindgut of each chimera showing the localization of EGFP (middle, green signal), PGC7 (middle and right, red signal) and laminin (middle, white line; right, white signal). Arrows indicate *Sox17*-null mutant ES cell-derived PGCs. White circles indicate *Sox17*-null mutant ES cell-derived gut endoderm. hg, hindgut. Bars are 50μm.

Table 3-1. **Contribution of *Sox17*-null ES cells to PGCs in 9.0 dpc chimeric embryos**

Sample	Donor ES / Distribution	wildtype (+/+)	*Sox17*-null (-/-)	Total
Wild (n=2)	hindgut	109 (96%)	0 (0%)	109 (96%)
	yolk sac	4 (4%)	0 (0%)	4 (4%)
Chimera (n=4)	hindgut	30 (10%)	265 (88%)	295 (98%)
	yolk sac	0 (0%)	7 (2%)	7 (2%)

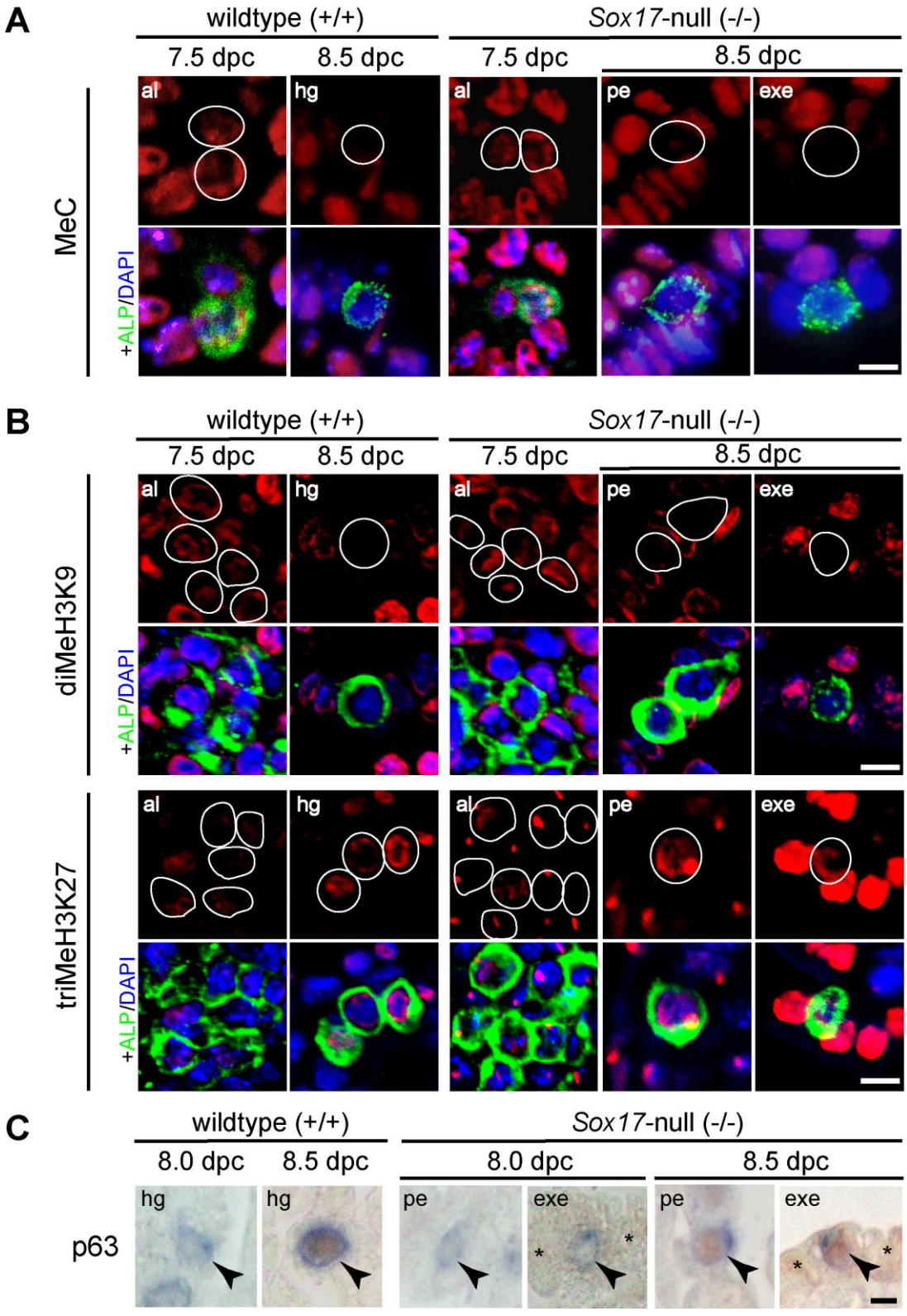

Figure 3-7. **Proper progression of p63 expression, DNA demethylation and histone modifications in the ectopic PGCs of *Sox17*-null embryos**

(A,) Methylated cytosine (MeC) status (red) with ALP (green, lower panels) and DAPI staining (blue, lower panels) in PGCs (white circles in upper panels; green signals in lower panels) of wildtype (+/+) and *Sox17*-null embryos (-/-). (B) diMeH3K9 (red) and triMeH3K27 status (red) with ALP (green, lower panels) and DAPI staining (blue, lower panels) in PGCs (white circles in upper panels; green signals in lower panels) of wildtype (+/+) and *Sox17*-null embryos (-/-). (C) p63 immunostaining (brown) with ALP staining (blue) in PGCs (arrowheads) of wildtype (+/+) and *Sox17*-null embryos (-/-). Asterisks indicate background in the visceral endoderm. al, base of allantois; exe, extraembryonic visceral endoderm; hg, embryonic hindgut endoderm; pe, presumptive embryonic endoderm. Bars are 10μm.

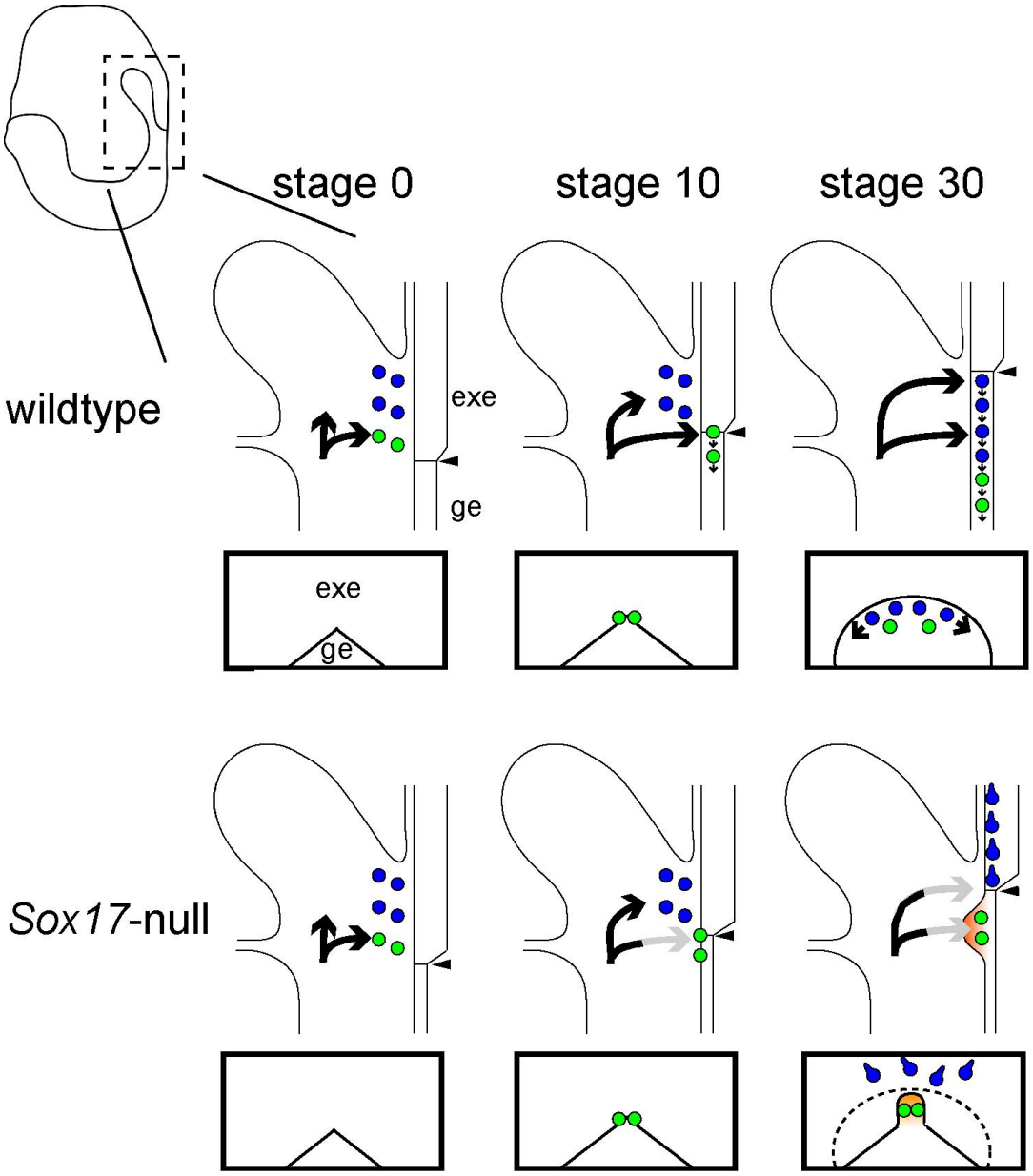

Figure 3-8. **Comparison of the PGCs migration and the expansion of newly-supplied embryonic hindgut endoderm in wildtype and *Sox17*-null embryos.**

In the *Sox17*-null embryos, a front population of the PGCs (green cells) is immobile within the presumptive embryonic endoderm (brown area), but the remaining PGCs

ectopically migrate away into the yolk sac endoderm in *Sox17*-null embryos (blue). By contrast, supply of wildtype embryonic hindgut endoderm cells can rescue defective migration of the *Sox17*-null PGCs by chimera analysis (Fig.3-6; Table 3-1). These results strongly suggest that the continuous supply and expansion of embryonic hindgut endoderm cells is essential for the PGCs movement into the correct path to the GRs. Black arrows indicate supply of embryonic hindgut endoderm via primitive streak. Gray arrows indicate impaired supply of embryonic hindgut endoderm in *Sox17*-null embryo.

exe, extraembryonic endoderm; ge, embryonic gut endoderm.

4. General Discussion

The germline, uniquely amongst the lineages of the embryo, carries the genome from generation to generation and is therefore the only lineage which retains true developmental totipotency. Migrating PGCs gradually acquire the germness by the celluer dynamics associated with the genome-wide epigenetic reprogramming (Seki *et al.,* 2005; 2007; Sasaki and Matsui, 2008). These modifications may be regulated by a cell-autonomous manner, and not by the localization within the embryonic hindgut endoderm environment (this study). Interestingly, *in vivo* PGCs potentially give rise to EC cells, pluripotent stem cells of teratomas, and eventually may become benign tumors containing derivatives of the three primary germ layers (Stevens, 1967). Similarly, PGCs can be converted into EG cells *in vitro*, pluripotent stem cells capable of giving rise to somatic and germline chimeras (Matsui *et al.*, 1992; Resnick *et al.*, 1992). The ability of PGCs to form EC cells *in vivo* and EG cells *in vitro* suggests that developmental potency of PGCs is essentially regulative to acquire pluripotency. During regionalization of PGCs within the embryonic hindgut endoderm, the hindgut endoderm environment may guard the migrating PGCs from abnormal aquirement of pluripotency until GRs formation.

It is commonly observed that ectopic PGCs appear during the active directional migration periods. Ectopic PGCs are first found in the allantois and the extraembryonic visceral endoderm layer during the migration period out of the primitive streak (Anderson *et al*., 2000; this study), and then in the dorsal body wall and organs surrounding the gonad at later stages of migration (Upadhyay and

Zamboni, 1982). Most of these ectopic PGCs are thought to undergo cell death, but the consequence of their survival could be detrimental. Nearly 3% of malignant pediatric tumors are germ cell tumors. More than 50% of these, and 18% of adult germ cell tumors, arise outside the gonad (Göbel *et al.*, 2000). They are presumed to arise from ectopic PGCs that failed to undergo cell death (Schneider *et al.*, 2001). Interestingly, ectopic PGCs are not likely to be generated in the period of PGCs migtration within the embryonic hindgut endoderm (Runyan *et al.*, 2008). From the present study, it is implied that the supply and expansion of the embryonic endoderm through the PGCs entry site is essential for PGCs movement into embryonic body. In other words, the “PGCs entry site” acts strictly as the first gate for the correct path of PGCs movement toward GRs during embryogenesis. In addition, I also provide the direct evidence for the crucial function of hindgut endoderm as a “coveyer belt” of the PGCs transport system. These knowledgements clearly indicate the essential role of the embryonic hindgut endoderm for correct PGCs migration arriving within the range of signals that are in leading to the GRs.

In many invertebrates and vertebrates, the formation of PGCs is spatially and temporally separated from the somatic gonad, and formed PGCs migrate from the original site to the future GRs during development. The regulation of PGCs behavior by the endodermal tissue during the early migrating period is not peculiar in mice. Despite the anatomical differences among the embryos, the principle path of mouse PGCs is similar to that of *Rana pipiens*, *Drosophila* and *C.elegans*. In these species,

after PGCs formation, PGCs pass through the endodermal tissue and then arrive within the range of guidance cues to the GRs such as SDF-1 (Ara *et al.,* 2003; Molyneaux *et al.,* 2003) and HMGCoAr (3-hydroxy-3-methylglutaryl coenzyme A reductase) (Van Doren *et al.,* 1998). In *Rana pipiens*, it has been shown that, although PGCs have inherent migratory properties, they do not leave the endoderm until morphogenesis occurs in their endodermal environment (Subtelny and Penkala, 1984). In *Drosophila*, it was proposed that PGCs are passively incorporated into the posterior midgut and initiate motility between stages 10 and 11, when they crawl out of the gut, which is observed morphologically (Warrior, 1994). This process may be initiated by changes in the epithelium of the midgut because the mutation that perturbs midgut formation prevented PGCs from assuming migratory cell shape (Jaglarz and Howard, 1995). Similar events occur in *C.elegans*. Germ cell (P_4) follows the neighboring two gut endodermal cells into the inward of the embryo during gastrulation (Sulston *et al.*, 1983). P_4 does not migrate interior in embryos when the migration of gut endodermal cells is inhibited (Powell-Coffman *et al.*, 1996). Taken together, the regulation of germ-line migration into the embryonic body by the endodermal tisssue during gastrulation is conserved even among insects, amphibians and mammals.

Interestingly, unlike mice, the PGCs of birds migrate to the GRs primarily by means of the bloodstream (Swift, 1914; Kuwana, 1993; Tsunekawa *et al.*, 2000). In birds, the PGCs are derived from epiblast cells that migrate from the crescent region of the area pellucida to a crescent-shaped zone in the hypoblast at the anterior

border of the area pellucida. This extraembryonic region is called the germinal crescent, and the PGCs multiply there. When blood vessels form in the germinal crescent, the PGCs enter those vessels and are carried by the circulation to the region where the hindgut is forming. Here they leave the circulation, become associated with the mesentery, and migrate into the GRs. This passive PGCs movement by the force of the bloodstream circulation seems to act as the environment to PGCs for waiting the GRs formation in the embryonic body. In this aspect, it could be considerd that the bloodstream in bird embryogenesis and the embryonic hindgut endoderm expansion in mouse embryogenesis play a similar role in directing PGCs movement to the GRs in both species.

In conclusion, I revealed the crucial function of the embryonic hindgut endoderm as the “PGCs entry site” and the “conveyor belt” of the PGCs transport system in mouse embryogeneisis (Fig. 4-1). These roles of the embryonic hindgut endoderm are essential for directing proper migration of maturating PGCs to GRs in mouse embryogenesis. Furthermore, my findings highlight that the regulation of germ-line migration by the gut endoderm during gastrulation is evolutionally conserved among invertebrates and mammals. This study elaborately provides a groundbreaking finding that the early embryonic gut morphogenesis strictly orchestrates germ cell development, which transmits genetic information to the next generation.

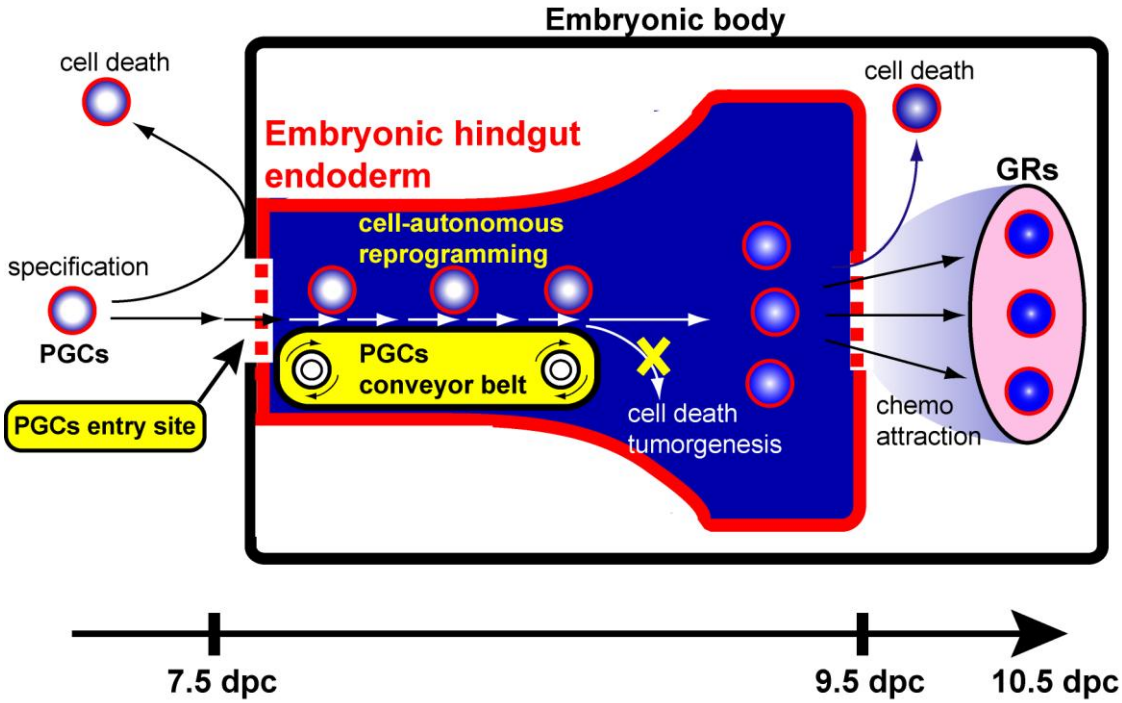

Figure 4-1. **Schematic representation of possible roles of embryonic hindgut endoderm in germ cell development.**

Crucial functions of the embryonic hindgut endoderm are the **"PGCs entry site"** into the embryonic body and the **"conveyor belt"** for the directing proper migration of PGCs to the GRs in mouse embryogenesis.

5. Summary

During mouse gastrulation, primordial germ cells (PGCs) appear and aggregate in the posterior primitive streak position at the base of allantois. PGCs then move caudally into the newly-forming hindgut endoderm before their entering the genital ridges. Although this migratory path of PGCs via endodermal soma is conserved among various animal species including *C. elegans* and *Drosophila*, the precise role of the endodermal cells in PGCs migration and differentiation remains unclear. Here I provide the direct evidence for crucial roles of the hindgut endoderm in directing proper PGCs migration, not epigenetic maturation, during late gastrulation to early somite stages. The *Sox17*-null mouse embryos displayed early and specific defects in hindgut expansion during late gastrulation. In these *Sox17*-null embryos, PGCs normally differentiated at the base of allantois, and then only a small number of the front PGCs population could move properly into the presumptive endodermal area. However, possibly due to defective expansion of *Sox17*-null endoderm, these PGCs in endodermal position were blocked to migrate from the primitive streak position into the outer layer of definitive endoderm throughout gastrulation. At the same time, a large number of remaining PGCs migrated away from the primitive streak into the ectopic position of the yolk sac visceral endoderm, where these ectopic cells properly progressed to epigenetic maturation similar to those of wildtype PGCs in hindgut. Chimera analysis of *Sox17*-null ES cells confirmed that the supply of wildtype endoderm cells can rescue defective migration of the *Sox17*-null PGCs into the proper hindgut position. The present results, therefore, imply that defective embryonic hindgut endoderm

expansion promotes ectopic PGCs migration into yolk sac visceral endoderm, highlighting the importance of the continuous supply and expansion of definitive endoderm cells for the selection of the PGCs into the correct path to the GRs. Furthermore, my findings highlight that the regulation of germ-line migration by the gut endoderm during gastrulation is evolutionally conserved among some invertebrates and mammals.

6. Acknowledgements

I wish to express profound thanks to Prof. Dr. Masamichi Kurohmaru (University of Tokyo), Associate Prof. Dr. Yoshiakira Kanai (University of Tokyo), Assistant Prof. Dr. Naoki Tsunekawa (University of Tokyo), and Dr. Masami Kanai-Azuma (Kyorin University) for their valuable guidance, encouragement and supports in the course of this study.

I wish to thank Associate Prof. Dr. Hiroshi Sasada (University of Tohoku), and Associate Prof. Hiromichi Matsumoto (University of Utsunomiya), Dr. Yasuyuki Abe (Obihiro University of Agriculture and Veterinary Medicine), Prof. Dr. Eimei Sato (University of Tohoku), Associate Prof. Dr. Masayoshi Kuwahara (University of Tokyo) and Prof. Dr. Yoshihiro Hayashi (University of Tokyo) for showing me the way of being a scientist and a man should be. I wish to thank to Prof. Dr. Atsuo Ogura (RIKEN BRC and University of Tokyo), Associate Prof. Dr. Satoshi Tanaka (University of Tokyo), and Associate Prof. Dr. Shigeru Kyuwa (University of Tokyo), for their critical reading of the manuscript. I wish to thank Prof. Dr. Yasuhisa Matsui (University of Tohoku) and Assistant Prof. Dr. Daiji Okamura (University of Tohoku) for providing the PGC7 antibody and Assistant Prof. Dr. Satomi Tanaka (University of Kumamoto) for providing the *Ifitm3 in situ* probe. I wish to thank Dr. Choji Taya, Dr. Hiroshi Shitara, Miss Rie Ishii and Dr. Hiromichi Yonekawa (The Tokyo Metropolitan Institute of Medical Science) for the technical assistance of chimeric analyses. I wish to thank Prof. Dr. Hayato Kawakami (Kyorin University) and Mr. Minoru Fukuda (Kyorin University) for the instructions in the use of electron microscopy.

I was able to enjoy my studying in Vet. Anat. Lab. with a pleasure because of Ms.

Kyoko Harikae, Mr. Ryuji Hiramatsu, Mr. Shogo Matoba, Assistant Prof. Dr. Toshiyasu Matsui, Mr. Yohei Sakamoto, Ms. Mami Uemura, Ms. Asuka Yoneda and Ms. Yoko Watanabe's kind and helpful advice for my foolish behaviors. I wish to thank Mrs. Itsuko Yagihashi for secretarial assistance and her grateful care of my mind. I will never forget all the members of Vet. Anat. Lab. for their grateful support during the course of the study.

Finally, I would like to express appreciation to my loving parents (Toshiyuki and Chisato Hara), brothers (Kojiro and Toshiro Hara), grandparents (Yukio and Kiyoko Hara; Masaharu and Kimiko Hiraki) and all friends for their grateful supports on my mind. I will never forget their love and kindness as long as I live.

7. References

Anderson R, Copeland TK, Schöler H, Heasman J, Wylie C. The onset of germ cell migration in the mouse embryo. Mech. Dev. 2000 91, 61-8.

Ara T, Nakamura Y, Egawa T, Sugiyama T, Abe K, Kishimoto T, Matsui Y, Nagasawa T. Impaired colonization of the gonads by primordial germ cells in mouse lacking a chemokine, stromal cell-derived factor-1 (SDF-1). Proc Natl Acad Sci U S A. 2003 100, 5319-23.

Besmer P, Manova K, Duttlinger R, Huang EJ, Packer A, Gyssler C, Bachvarova RF. The kit-ligand (steel factor) and its receptor c-kit/W: pleiotropic roles in gametogenesis and melanogenesis. Dev. Suppl. 1993 125-37. Review.

Bielinska, M., Narita, N. and Wilson, D. B. Distinct roles for visceral endoderm during embryonic mouse development. Int. J. Dev. Biol. 1999 43, 183-205.

Bowles J, Schepers G, Koopman P. Phylogeny of the SOX family of developmental transcription factors based on sequence and structural indicators. Dev. Biol. 2000 227, 239-55. Review.

Buehr M, McLaren A, Bartley A, Darling S. Proliferation and migration of primordial germ cells in We/We mouse embryos. Dev. Dyn. 1993 198, 182-9.

Cermenati S, Moleri S, Cimbro S, Corti P, Del Giacco L, Amodeo R, Dejana E,

Koopman P, Cotelli F, Beltrame M. Sox18 and Sox7 play redundant roles in vascular development. Blood. 2008 111, 2657-66.

Chuma S, Nakatsuji N. Autonomous transition into meiosis of mouse fetal germ cells in vitro and its inhibition by gp130-mediated signaling. Dev. Biol. 2001 229, 468-79.

Ciruna B, Rossant J. FGF signaling regulates mesoderm cell fate specification and morphogenetic movement at the primitive streak. Dev. Cell 2001 1, 37-49.

Clark JM, Eddy EM. Fine structural observations on the origin and associations of primordial germ cells of the mouse. Dev. Biol. 1975 47, 136-55.

de Jong J, Stoop H, Gillis AJ, van Gurp RJ, van de Geijn GJ, Boer M, Hersmus R, Saunders PT, Anderson RA, Oosterhuis JW, Looijenga LH. Differential expression of SOX17 and SOX2 in germ cells and stem cells has biological and clinical implications. J. Pathol. 2008 215, 21-30

Doitsidou M, Reichman-Fried M, Stebler J, Köprunner M, Dörries J, Meyer D, Esguerra CV, Leung T, Raz E. Guidance of primordial germ cell migration by the chemokine SDF-1. Cell 2002 111, 647-59.

Donovan PJ, Stott D, Cairns LA, Heasman J, Wylie CC. Migratory and postmigratory mouse primordial germ cells behave differently in culture. Cell 1986 44, 831-8.

Dunn TL, Mynett-Johnson L, Wright EM, Hosking BM, Koopman PA, Muscat GE. Sequence and expression of Sox-18 encoding a new HMG-box transcription factor. Gene 1995 161, 223-5.

Göbel U, Schneider DT, Calaminus G, Haas RJ, Schmidt P, Harms D. Germ-cell tumors in childhood and adolescence. GPOH MAKEI and the MAHO study groups. Ann. Oncol. 2000 11, 263-71. Review.

Hart AH, Hartley L, Sourris K, Stadler ES, Li R, Stanley EG, Tam PP, Elefanty AG, Robb L. Mixl1 is required for axial mesendoderm morphogenesis and patterning in the murine embryo. Development 2002 129, 3597-608.

Heasman J, Wylie CC. Contact relations and guidance of primordial germ cells on their migratory route in embryos of Xenopus laevis. Proc. R Soc. Lond. B Biol. Sci. 1981 213, 41-58.

Herpin A, Fischer P, Liedtke D, Kluever N, Neuner C, Raz E, Schartl M. Sequential SDF1a and b-induced mobility guides Medaka PGC migration. Dev. Biol. 2008 320, 319-27.

Jaglarz MK, Howard KR. The active migration of Drosophila primordial germ cells. Development 1995 121, 3495-503.

Kanai Y, Kanai-Azuma M, Noce T, Saido TC, Shiroishi T, Hayashi Y, Yazaki K. Identification of two Sox17 messenger RNA isoforms, with and without the high mobility group box region, and their differential expression in mouse spermatogenesis. J. Cell Biol. 1996 133, 667-81.

Kanai Y, Koopman P. Structural and functional characterization of the mouse Sox9 promoter: implications for campomelic dysplasia. Hum. Mol. Genet. 1999 8, 691-6.

Kanai-Azuma M, Kanai Y, Okamoto M, Hayashi Y, Yonekawa H, Yazaki K. Nrk: a murine X-linked NIK (Nck-interacting kinase)-related kinase gene expressed in skeletal muscle. Mech. Dev. 1999 89, 155-9.

Kanai-Azuma M, Kanai Y, Gad JM, Tajima Y, Taya C, Kurohmaru M, Sanai Y, Yonekawa H, Yazaki K, Tam PP, Hayashi Y. Depletion of definitive gut endoderm in *Sox17*-null mutant mice. Development 2002 129, 2367-79.

Kim I, Saunders TL, Morrison SJ. Sox17 dependence distinguishes the transcriptional regulation of fetal from adult hematopoietic stem cells. Cell 2007 130, 470-83.

Kurimoto K, Yabuta Y, Ohinata Y, Shigeta M, Yamanaka K, Saitou M. Complex genome-wide transcription dynamics orchestrated by Blimp1 for the specification of the germ cell lineage in mice. Genes Dev. 2008 22, 1617-35.

Kuwana T. Migration of avian primordial germ cells toward the gonadal anlage. Dev. Growth Diff. 1993 35, 237-43.

Kwon GS, Viotti M, Hadjantonakis AK. The endoderm of the mouse embryo arises by dynamic widespread intercalation of embryonic and extraembryonic lineages. Dev. Cell 2008 15, 509-20.

Lange UC, Adams DJ, Lee C, Barton S, Schneider R, Bradley A, Surani MA. Normal germ line establishment in mice carrying a deletion of the Ifitm/Fragilis gene family cluster. Mol. Cell Biol. 2008 28, 4688-96.

Lawson KA, Meneses JJ, Pedersen RA. Clonal analysis of epiblast fate during germ layer formation in the mouse embryo. Development. 1991 113, 891-911.

Lawson KA, Dunn NR, Roelen BA, Zeinstra LM, Davis AM, Wright CV, Korving JP, Hogan BL. Bmp4 is required for the generation of primordial germ cells in the mouse embryo. Genes Dev. 1999 13, 424-36.

Lefebvre V, Dumitriu B, Penzo-Méndez A, Han Y, Pallavi B. Control of cell fate and differentiation by Sry-related high-mobility-group box (Sox) transcription factors. Int J. Biochem. Cell Biol. 2007 39, 2195-214. Review.

Maatouk DM, Resnick JL. Continuing primordial germ cell differentiation in the mouse

embryo is a cell-intrinsic program sensitive to DNA methylation. Dev. Biol. 2003 258, 201-8.

Matsui T, Kanai-Azuma M, Hara K, Matoba S, Hiramatsu R, Kawakami H, Kurohmaru M, Koopman P, Kanai Y. Redundant roles of Sox17 and Sox18 in postnatal angiogenesis in mice. J. Cell Sci. 2006 119, 3513-26.

Matsui Y, Zsebo K, Hogan BL. Derivation of pluripotential embryonic stem cells from murine primordial germ cells in culture. Cell 1992 70, 841-7.

McLaren A, Lawson KA. How is the mouse germ-cell lineage established? Differentiation 2005 73, 435-7. Review.

McLaren A, Southee D. Entry of mouse embryonic germ cells into meiosis. Dev. Biol. 1997 187, 107-13.

Molyneaux KA, Stallock J, Schaible K, Wylie C. Time-lapse analysis of living mouse germ cell migration. Dev. Biol. 2001 240, 488-98.

Molyneaux KA, Zinszner H, Kunwar PS, Schaible K, Stebler J, Sunshine MJ, O'Brien W, Raz E, Littman D, Wylie C, Lehmann R. The chemokine SDF1/CXCL12 and its receptor CXCR4 regulate mouse germ cell migration and survival. Development 2003 130, 4279-86.

Molyneaux K, Wylie C. Primordial germ cell migration. Int. J. Dev. Biol. 2004 48, 537-44.

Nakamuta N, Kobayashi S. Expression of p63 in the mouse primordial germ cells. J. Vet. Med. Sci. 2004 66, 1365-70.

Ohbo K, Yoshida S, Ohmura M, Ohneda O, Ogawa T, Tsuchiya H, Kuwana T, Kehler J, Abe K, Schöler HR, Suda T. Identification and characterization of stem cells in prepubertal spermatogenesis in mice. Dev. Biol. 2003 258, 209-25.

Ohkubo Y, Shirayoshi Y, Nakatsuji N. Autonomous regulation of proliferation and growth arrest in mouse primordial germ cells studied by mixed and clonal cultures. Exp. Cell Res. 1996 222, 291-7.

Ohinata Y, Payer B, O'Carroll D, Ancelin K, Ono Y, Sano M, Barton SC, Obukhanych T, Nussenzweig M, Tarakhovsky A, Saitou M, Surani MA. Blimp1 is a critical determinant of the germ cell lineage in mice. Nature 2005 436, 207-13.

Powell-Coffman JA, Knight J, Wood WB. Onset of C. elegans gastrulation is blocked by inhibition of embryonic transcription with an RNA polymerase antisense RNA. Dev. Biol. 1996 178, 472-83.

Resnick JL, Bixler LS, Cheng L, Donovan PJ. Long-term proliferation of mouse

primordial germ cells in culture. Nature. 1992 359, 550-1.

Saitou M, Barton SC, Surani MA. A molecular programme for the specification of germ cell fate in mice. Nature 2002 418, 293-300.

Sakamoto Y, Hara K, Kanai-Azuma M, Matsui T, Miura Y, Tsunekawa N, Kurohmaru M, Saijoh Y, Koopman P, Kanai Y. Redundant roles of Sox17 and Sox18 in early cardiovascular development of mouse embryos. Biochem. Biophys. Res. Commun. 2007 360, 539-44.

Sasaki H, Matsui Y. Epigenetic events in mammalian germ-cell development: reprogramming and beyond. Nat. Rev. Genet. 2008 9, 129-40. Review.

Sato M, Kimura T, Kurokawa K, Fujita Y, Abe K, Masuhara M, Yasunaga T, Ryo A, Yamamoto M, Nakano T. Identification of PGC7, a new gene expressed specifically in preimplantation embryos and germ cells. Mech. Dev. 2002 113, 91-4.

Schneider DT, Schuster AE, Fritsch MK, Hu J, Olson T, Lauer S, Göbel U, Perlman EJ. Multipoint imprinting analysis indicates a common precursor cell for gonadal and nongonadal pediatric germ cell tumors. Cancer Res. 2001 61, 7268-76.

Schöler HR, Ruppert S, Suzuki N, Chowdhury K, Gruss P. New type of POU domain

in germ line-specific protein Oct-4. Nature 1990 344, 435-9.

Seki Y, Hayashi K, Itoh K, Mizugaki M, Saitou M, Matsui Y. Extensive and orderly reprogramming of genome-wide chromatin modifications associated with specification and early development of germ cells in mice. Dev. Biol. 2005 278, 440-58.

Seki Y, Yamaji M, Yabuta Y, Sano M, Shigeta M, Matsui Y, Saga Y, Tachibana M, Shinkai Y, Saitou M. Cellular dynamics associated with the genome-wide epigenetic reprogramming in migrating primordial germ cells in mice. Development 2007 134, 2627-38.

Shimoda M, Kanai-Azuma M, Hara K, Miyazaki S, Kanai Y, Monden M, Miyazaki J. Sox17 plays a substantial role in late-stage differentiation of the extraembryonic endoderm in vitro. J. Cell Sci. 2007 120, 3859-69.

Sohn J, Natale J, Chew LJ, Belachew S, Cheng Y, Aguirre A, Lytle J, Nait-Oumesmar B, Kerninon C, Kanai-Azuma M, Kanai Y, Gallo V. Identification of Sox17 as a transcription factor that regulates oligodendrocyte development. J. Neurosci. 2006 26, 9722-35.

Stallock J, Molyneaux K, Schaible K, Knudson CM, Wylie C. The pro-apoptotic gene Bax is required for the death of ectopic primordial germ cells during their migration

in the mouse embryo. Development 2003 130, 6589-97.

Stebler J, Spieler D, Slanchev K, Molyneaux KA, Richter U, Cojocaru V, Tarabykin V, Wylie C, Kessel M, Raz E. Primordial germ cell migration in the chick and mouse embryo: the role of the chemokine SDF-1/CXCL12. Dev. Biol. 2004 272, 351-61.

Stevens LC. Origin of testicular teratomas from primordial germ cells in mice. J. Natl. Cancer Inst. 1967 38, 549-52.

Sturm K, Tam PP. Isolation and culture of whole postimplantation embryos and germ layer derivatives. Methods. Enzymol. 1993 225, 164-90.

Subterny S, Penkala JE. Experimental evidence for a morphogenetic role in the emergence of primordial germ cells from the endoderm in Rana pipiens. Differentiation 1984 26, 211-219.

Suh EK, Yang A, Kettenbach A, Bamberger C, Michaelis AH, Zhu Z, Elvin JA, Bronson RT, Crum CP, McKeon F. p63 protects the female germ line during meiotic arrest. Nature 2006 444, 624-8.

Sulston JE, Schierenberg E, White JG, Thomson JN. The embryonic cell lineage of the nematode Caenorhabditis elegans. Dev. Biol. 1983 100, 64-119.

Swift CH. Origin and early history of the primordial germ-cells in the chick. Am. J. Anat. 1914 15, 483-516.

Tam PP, Beddington RS. The formation of mesodermal tissues in the mouse embryo during gastrulation and early organogenesis. Development 1987 99, 109-26.

Tam PP, Kanai-Azuma M, Kanai Y. Early endoderm development in vertebrates: lineage differentiation and morphogenetic function. Curr. Opin. Genet. Dev. 2003 13, 393-400. Review.

Tam PP, Khoo PL, Lewis SL, Bildsoe H, Wong N, Tsang TE, Gad JM, Robb L. Sequential allocation and global pattern of movement of the definitive endoderm in the mouse embryo during gastrulation. Development 2007 134, 251-60.

Tanaka SS, Matsui Y. Developmentally regulated expression of mil-1 and mil-2, mouse interferon-induced transmembrane protein like genes, during formation and differentiation of primordial germ cells. Gene Expr. Patterns 2002 2, 297-303.

Tanaka SS, Yamaguchi YL, Tsoi B, Lickert H, Tam PP. IFITM/Mil/fragilis family proteins IFITM1 and IFITM3 play distinct roles in mouse primordial germ cell homing and repulsion. Dev. Cell 2005 9, 745-56.

Taniguchi K, Hiraoka Y, Ogawa M, Sakai Y, Kido S, Aiso S. Isolation and

characterization of a mouse SRY-related cDNA, mSox7. Biochim. Biophys. Acta. 1999 14, 225-31.

Tsunekawa N, Naito M, Sakai Y, Nishida T, Noce T. Isolation of chicken vasa homolog gene and tracing the origin of primordial germ cells. Development 2000 127, 2741-50.

Upadhyay S, Zamboni L. Ectopic germ cells: natural model for the study of germ cell sexual differentiation. Proc. Natl. Acad. Sci. U S A 1982 79, 6584-8.

Van Doren M, Broihier HT, Moore LA, Lehmann R. HMG-CoA reductase guides migrating primordial germ cells. Nature 1998 396, 466-9.

Warrior R. Primordial germ cell migration and the assembly of the Drosophila embryonic gonad. Dev. Biol. 1994 166, 180-94.

Whitington PM, Dixon KE. Quantitative studies of germ plasm and germ cells during early embryogenesis of Xenopus laevis. J. Embryol. Exp. Morphol. 1975 33, 57-74.

Wilson V, Beddington RS. Cell fate and morphogenetic movement in the late mouse primitive streak. Mech. Dev. 1996 55, 79-89.

Yabuta Y, Kurimoto K, Ohinata Y, Seki Y, Saitou M. Gene expression dynamics during

germline specification in mice identified by quantitative single-cell gene expression profiling. Biol. Reprod. 2006 75, 705-16.

Yamaguchi S, Kimura H, Tada M, Nakatsuji N, Tada T. Nanog expression in mouse germ cell development. Gene Expr. Patterns 2005 5, 639-46.

Ying Y, Liu XM, Marble A, Lawson KA, Zhao GQ. Requirement of Bmp8b for the generation of primordial germ cells in the mouse. Mol. Endocrinol. 2000 14, 1053-63.